



TECHNISCHE
UNIVERSITÄT
WIEN

Diplomarbeit

**Study of optimal speed planning and
energy management for eco-driving of
fuel cell electric trucks**

ausgeführt um Zwecke der Erlangung des
akademischen Grades

Diplom-Ingenieur

eingereicht an der

Technische Universität Wien

**Fakultät für Maschinenwesen und
Betriebswissenschaften**

unter der Leitung von
Associate Prof. Dr. techn. Christoph Hametner

von

Javier Lopez Ortiz, BSc.

Matrikelnummer: 12019249

Ich habe zur Kenntnis genommen, dass ich zur Drucklegung meiner Arbeit unter der Bezeichnung

Study of optimal speed planning and energy management for eco-driving of fuel cell electric trucks

nur mit Bewilligung der Prüfungskommission berechtigt bin.

Ich erkläre weiters Eides statt, dass ich meine Diplomarbeit nach den anerkannten Grundsätzen für wissenschaftliche Abhandlungen selbstständig ausgeführt habe und alle verwendeten Hilfsmittel, insbesondere die zugrunde gelegte Literatur, genannt habe. Weiters erkläre ich, dass ich dieses Diplomarbeitsthema bisher weder im In- noch Ausland (einer Beurteilerin/einem Beurteiler zur Begutachtung) in irgendeiner Form als Prüfungsarbeit vorgelegt habe und dass diese Arbeit mit der vom Begutachter beurteilten Arbeit übereinstimmt.

Abstract

The increase in greenhouse emissions from the road freight transport sector has encouraged the search for new, cleaner, and more sustainable alternatives in order to achieve the European goals for environmental pollution. One of the alternatives that is beginning to be established is the use of hydrogen fuel cells and electric batteries as energy sources for electric motors. Fuel cell electric trucks have the great advantage of being able to make long-distance trips with one single recharge, with a similar range to conventional combustion cars, but without emitting polluting gases into the atmosphere.

This master's thesis focuses on the study of the optimal speed planning and energy management control of a fuel cell electric truck in realistic scenarios. The final goals are to minimize these terms depending on the road topography and the trip time and analyse their trade-off over driving time. Dynamic programming is the method adopted in this work to solve the optimal control problem and ensure the global optimality. However, one of the drawbacks of solving the optimization by dynamic programming is the curse of dimensionality when multiple state and control variables are added to the problem increasing the computational burden. For this reason, it is used a hierarchical strategy instead of a co-optimization of the two problems, decreasing the high complexity of the optimal control problem. Hierarchical optimization split the global control problem into two sub-problems: optimal speed-planning control and energy management control. Speed planning provides the optimal speed distribution along the route to minimize the total energy consumption of the truck, using the elevation profile as input. Energy management uses the speed and power profile data from the speed planning, and it calculates the optimal distribution of fuel cell and battery power to the powertrain. Speed planning control is optimized under motorway speed limits and power motor constraints and the energy management control under fuel cell and battery power limits and the degradation of the battery based on the state of charge. It is also analysed the behaviour of the battery based on the energy released by the internal ohmic resistance of the battery, called ohmic losses. High ohmic losses lead to high temperature which must be managed by the battery thermal management system to reduce the degradation of the components. The thesis shows simulations from different scenarios, varying the load of the truck, using different elevation profiles, as well as penalizing high power motor values and implementing different strategies in the optimal speed planning and energy management control.

From the results, it is observed that the optimal speed planning avoids mechanical braking and increases the use of coasting to reduce energy consumption. In addition, it is shown that including ohmic terms in the objective function improve battery behaviour without a significant impact in energy or hydrogen consumption. Future works should model in detail the fuel cell system of the truck considering hydrogen consumption due to high gradients in the fuel cell power, curves of the road, and the design of an online control of the truck in real-time.

Acknowledgements

This master's thesis would not be possible without the invaluable support of my family and friends who have always been with me during this year. I would also like to thank Alessandro Ferrara for his feedback and help in every step of the thesis.

Content

1. Introduction	1
1.1. Motivation	1
1.1.1. Transition from ICE to battery electric and fuel cell electric vehicles	3
1.2. Literature Survey	8
1.3. Contribution	11
1.4. Outline	12
2. Background	13
2.1. Vehicle Modelling	13
2.1.1. Vehicle dynamics	13
2.1.2. Fuel cell system	15
2.1.3. Battery system	16
2.1.4. Parameters and constraints of the vehicle	20
2.2. Driving cycles	21
2.3. Dynamic programming	23
2.3.1. Dynamic programming formulation	23
2.3.2. Curse of dimensionality	25
3. Optimal Speed Planning and Energy Management	27
3.1. Optimization	27
3.1.1. Cost function optimal speed planning	28
3.1.2. Cost function energy management	30
3.1.3. Constraints in the optimization	31
3.1.4. Discretization of dynamic programming variables	32
3.2. Strategies to solve the optimization	33
3.2.1. Solve optimization problem by using directly dynamic programming .	34
3.2.2. Solve optimization problem by using the synthesis of Pontryagin's minimum principle	35
4. Results	36
4.1. Optimal speed planning overview	36
4.2. Evaluation of speed planning strategies	40
4.2.1. Comparison of the speed and power profile over the total route for both strategies	40
4.2.2. Evaluation of energy consumption and computational time for both strategies	41
4.3. Optimal speed planning and energy management results	42

4.3.1.	Analysis of results using power constraints	42
4.3.2.	Analysis of the effects of driving time over consumption	45
4.3.3.	Evaluation of results for different elevation profiles	47
4.3.4.	Analysis of results for different vehicle loads	49
4.3.5.	Evaluation of results using different objective functions in the optimal speed planning and energy management	52
5.	Conclusions	58
6.	Bibliography	61
7.	Appendix	66

List of Figures

Figure 1: Share of greenhouse emissions 2019, *Including international bunkers in transport emissions. Source:[3]	2
Figure 2: Powertrain of the fuel cell electric truck.....	13
Figure 3: Representation of resistances forces on the truck. Source: [40].....	15
Figure 4: Fuel cell system efficiency and hydrogen fuel cell mass respect to the fuel cell power. Source: [40].....	16
Figure 5: Scheme of the battery system. Source: [40].....	17
Figure 6: Representation of the battery pack in the vehicle.	17
Figure 7: Open Circuit Voltage over SoC.....	18
Figure 8: Representation of the resistance over SoC for both charge and discharge operation modes.....	19
Figure 9: Driving cycle (Uphill) from real data.	22
Figure 10: Driving cycle (Flat cycle) adjusted start and end elevation to zero	23
Figure 11: Scheme of the methodology used for the optimal speed planning and energy management	27
Figure 12: : Overview of the optimal speed planning results. Speed and power hard constraints are show by a black line and power linear constraints by a dash-line. Regenerative power limit is also shown in the electric motor power plot by the green dash-line.....	37
Figure 13: Behaviour similar than PnG for different slopes on the road from the optimal speed planning. Before the uphill the motor increases the electrical power and when the truck is almost at the top it starts the coasting.	38
Figure 14: Comparative of the use of the smooth term in both strategies.	39
Figure 15: Results profiles comparative between both strategies	40
Figure 16: Zoom of a section in both strategies.....	41
Figure 17: Comparison of motor energy consumption and computational time for both strategies.....	41
Figure 18: Optimal speed planning and energy management control results with and without soft power constraints at 250 kW.	43

Figure 19: Comparison of hydrogen consumption using soft power constraints and without power constraints.....	44
Figure 20: Comparison of ohmic losses using soft power constraints and without power constraints.....	45
Figure 21: Energy management results for different trip times	46
Figure 22: Trade-off energy consumption over time.....	46
Figure 23: Trade-off hydrogen consumption over time	47
Figure 24: Electric motor energy consumption on an uphill and a flat route.....	48
Figure 25: Hydrogen consumption on an uphill and flat route.....	48
Figure 26: Ohmic losses on an uphill and flat route.....	49
Figure 27: Electric motor energy for different vehicle loads	50
Figure 28: Ohmic losses for different vehicle loads	51
Figure 29: Hydrogen consumption for different vehicle loads	51
Figure 30: Comparison of hydrogen consumption respect to a full load 40 tonnes for a trip time of 52,5 min	51
Figure 31: Comparison of profiles for full and partial vehicle loads.	52
Figure 32: Hydrogen consumption results for different objectives functions in the speed planning.....	54
Figure 33: Ohmic losses for different objectives functions in the speed planning.....	54
Figure 34: Hydrogen consumption results for different objectives functions in the energy management.	56
Figure 35: Ohmic losses results for different objectives functions in the energy management.....	56

1. Introduction

This master's thesis aims to provide a new insight into the energy and hydrogen consumption of a fuel cell electric truck. To justify the need for this study and the implementation of the optimal control, it is explained the impact of the heavy-duty transport on greenhouse emissions, the transition and characteristics of different vehicle powertrains, the current literature available on this topic, and finally, the contribution.

1.1. Motivation

Transport is considered one of the major contributors to the formation of basic pollutants such as nitrogen oxides NO_x, suspended particles, carbon oxides, or sulfur dioxide SO₂. It also contributes significantly to greenhouse emissions by producing CO₂, N₂O, and CH₄, and enhances the formation of smog as chemical pollution of the atmosphere. These components affect human health, reduce buildings service life, and increase eutrophication. [1, 2]. According to [3] the top three activities producing greenhouse emissions are transport, energy supply, and industry, being transport the most contributor with 28.5% of the total CO₂ emissions. In a second breakdown of the transport emissions, it is observed that the road transportation is positioned as the main agent with 76.65% of the total emissions from this sector. Car passengers are by far the largest contributor to the road transport emissions, but heavy-duty trucks come in second position with 27.1%. These data, shown in Figure 1, give us a good perspective of the influence of this activity on the global greenhouse emissions and the importance of minimizing them.

In recent years all economic sectors attempt to minimize greenhouse emissions as much as possible to preserve the environment and reduce contamination. This is reflected in the Kyoto Protocol (2005) and the Paris Agreement (2015) to keep the average global temperature increase below at least 2°C and the warming below 1.5°C. In addition, several proposals have been adopted by the members of the European Parliament in order to reduce CO₂ emissions from new trucks by 15% by 2025, compared to 2019 levels. This improvement in CO₂ emissions must be continued till reaching a reduction of 30% in 2030 [1].

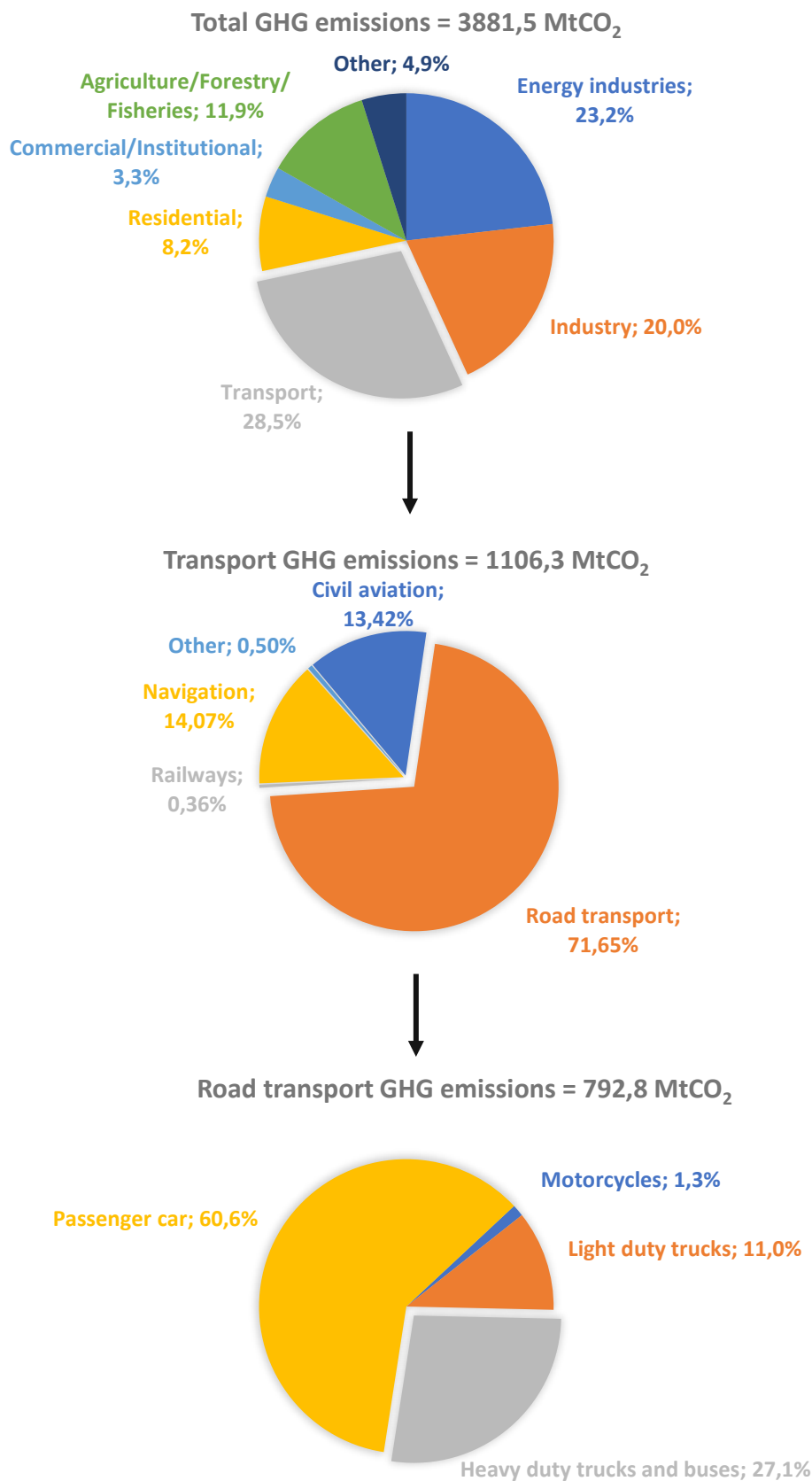


Figure 1: Share of greenhouse emissions 2019, *Including international bunkers in transport emissions.
Source:[3]

The last European Environmental Agency report shows a historic drop in the EU's greenhouse emissions over Europe. "The data confirms a 30-year downward trend which led to the EU achieving its 2020 target to reduce emissions by 20% compared to 1990 levels", reported the agency. This decrease in emissions is applied to almost every sector, but not to road transport. Road transport CO₂ emissions decreased by 123 million tonnes (-14%) from 2019 to 2020 due to a drastic reduction in transport activity resulting from the lockdown measures during the Covid-19 pandemic, but even at this level, the overview from 1990 is negative [4]. In addition, emissions of road freight transport raised again in 2021, when Covid restrictions were released, and the transport activity started working again as in previous years. The growth of the transport sector attached to the increase in the volume of the truck fleets on the roads, which contribute to 25% of the road transport emissions, arrives at the situation where European transport rises their emission levels despite improvements in engine efficiency, [5, 4].

To obtain a global idea about the contamination and emissions of the fuel used in vehicles, the whole life cycle from the extraction of the raw material to the final use must be taken into account, denoted as Well to Wheels (WTW). This cycle is split into Well to Tank (WTT), which encompasses the greenhouse gas production and energy intensity at the source-to-tank stage, and Tank to Wheels (TTW), regarding the emissions and energy intensity during vehicle operation. Conventional fuels as fossil fuels are obtained from the extraction of oil and natural gas as raw materials. On the other hand, to evaluate the emissions of electromobility must be considered the emissions from the electricity generation, reason why it is not a complete "zero-emission" mode of transport. In the coming years, it is expected by the EU to produce all the energy for the electromobility only from green sources minimizing the impact of the total cycle of emissions to almost zero. In addition, EU countries are highly dependent on China to obtain oil for fuel consumption. Prognoses suggest that China's dependency on foreign oil will exceed 80% by 2030 which would lead to a rise in transportation service prices, [1, 6].

Increments in greenhouse emissions and prices in conventional fuels enhance companies to develop and produce new transport vehicle models such as electric, hydrogen, or autonomous heavy-duty trucks, and the government to implement politics to benefit the use of these new models by building electric vehicle charging or hydrogen fuel stations.

1.1.1. Transition from ICE to battery electric and fuel cell electric vehicles

The increase in road freight transport and greenhouse gas emissions have gained the interest of researchers and vehicle companies to investigate alternative powertrain technologies for heavy-duty vehicles (HDVs). The first change of source for HDVs ICE was the transition from gasoline to diesel or compression ignition (CI) engines due to their greater energy efficiency. These heavy-duty vehicles need less fuel consumption, so transportation is cheaper. CI engines use diesel fuel which has

around 10-15 % more energy content than gasoline. The range of heavy-duty vehicles using diesel is around 975-1950 km, main reason why is mostly used in freight transport. Regarding energy efficiency, diesel has a specific energy of 42.9 MJ/kg, 43-44 % of energy efficiency, and the rest is converted into heat and friction. On the other hand, they present a significant drawback regarding emissions released during engine operation in comparison to gasoline or spike ignition (SI) engines [7, 8].

The next step is the transition from diesel to zero-emissions trucks. This transition must be guided by policy support from governments. They should actively be involved to speed up and promote the production of new vehicles with free pollution as well as the construction of the infrastructure necessary to achieve that. Battery electric and hydrogen fuel cell HDVs are two available alternatives to diesel engines. Vehicles using these batteries and fuel cells replace the ICE for an electric motor which is provided by the power from the chemical energy stored in active materials.

Electric vehicles consist of a battery power pack connected to a DC/AC inverter and an electric motor. The battery pack contains a battery management system to monitor the battery's state of charge (SOC), state of health (SOH), and state of energy (SOE). The powertrain of electric vehicles is simpler than ICE vehicles with an average of 60% fewer components, [9]. Apart from the simplicity of the electric vehicles, one other advantage is the regenerative braking capabilities to use certain energy from the wheels to the motor without losses in heat during the braking. The battery range for a typical passenger electric vehicle is around 330 km with some brands above 600 km as Lucid, or Mercedes, [10]. The range for BEV trucks class 8 decrease respect light battery vehicles with a current range average of about 150-200 km, [11]. The range of electric vehicles should increase for the feasibility of long hauls, so numerous vehicle manufacturers are working on second and third generations of their electric trucks, which will have increased ranges. The latest generation of the Volvo VNR Electric has a range of 275 km with a battery capacity of 565 kWh and the Nikola Motors TRE truck has an expected range of 563 km, with a battery capacity of 753kWh, [12, 13, 14]. These values depend on many different factors such as the elevation of the road, the vehicle weight or the average speed, but overall, it seems that there is a continuous improvement in BEV trucks range and feasibility for the coming years. Another drawback regarding battery electric trucks is the charging time. Type 3 charges along the road only provide 40 kW, which means that for a battery capacity of 565 kWh, it would take around 14 h to fully charge it, [15]. To solve this problem, companies are working on the production of new fast chargers such as Heliox with a charger up to 300 kW for battery electric trucks, [16]. Currently, the lack of infrastructure in electric stations with low-power chargers makes their feasibility difficult, but innovations and investments to build more stations with proper chargers could bring a bright future for battery electric trucks. The specific energy of Li-ion batteries could be around 120-220 Wh/kg with an efficiency between 64.4% and 86%, [17].

Hydrogen fuel cells are electromechanical energy devices that convert the chemical energy of hydrogen into electricity, heat, and water in a clean way without emissions. Hydrogen atoms from the fuel tank at the anode are ionized, then, the hydrogen

protons pass through the proton exchange membrane, where they react with oxygen and form water as a by-product. Meanwhile, the electrons stripped from the hydrogen fuel can be used to power the electric motors of the vehicle or charge the vehicle's battery. The powertrain of the fuel cell vehicles is similar to the electric battery vehicles. They both contain batteries and have their energy sources connected to electric motors that power their propulsion. Additionally, both have regenerative braking capabilities, which allow the batteries to be charged during decelerations or negative slopes on the road. The main difference between these vehicles is that while BEVs use batteries as their primary energy source, FCEVs employ fuel cell stacks and hydrogen, and batteries in these vehicles are used as energy buffers to make the fuel cell operation more efficient and regenerate braking energy. The range and recharge of hydrogen fuel cell vehicles are very similar to ICE vehicles. They can refuel in less than 4 minutes with a driving range of over 500 km. Recently, the range of the hydrogen HDVs are between 500 to 1000 km with a single fuelling session of two hydrogen tanks of 40-60 kg of hydrogen each one as the new Volvo trucks up to 1000 km with a refuelling time of less than 15 mins. The specific energy of hydrogen is around 32.702 kWh/kg with an efficiency of 51-59 % and they are designed to last the lifetime of the vehicle, about 25,000 h. HDVs drive an average. At the end of its lifespan, the fuel cell is disassembled, and the materials are recycled [18, 19, 7].

The large range of hydrogen HDV, enable and make them suitable for long distances even in countries where refuelling station are limited. However, fuel cells carry the disadvantage of lower power density and lower power response compared to other power sources. Another difference between batteries and fuel cells is that batteries have the active material stored within the system, while fuel cells have the active materials continuously fed into the system. BEV batteries are often composed of lithium-ion cells due to their high energy and power density. On the other hand, HFCVs often use proton exchange membrane fuel cells (PEMFC) due to their high-power density and cold-start capabilities [7]. A comparison of diesel, batteries, and hydrogen fuel cells is presented in Table 1.

Table 1: Comparison of different vehicles model

Criteria	Diesel	Battery	Hydrogen Fuel Cell
Well to tank	86% [20]	55% [20]	76% [20]
Tank to wheel	43% [21]	68% [21]	45% [21]
Range	1500-3200 km	200-600 km	~ 1000 km
Refuelling time	6-12 min	~ 3h	~15 min
Specific Energy	42MJ/kg	~ 0.81 MJ/kg	~ 117 MJ/kg

Recent studies developed a strategy where batteries, supercapacitors, and energy storage systems are used in conjunction with fuel cells to mitigate the disadvantages of fuel cells while maintaining the advantage of being a sustainable fuel source [7]. Nowadays, investigations of fuel cell hydrogen HDVs are still ongoing, and some companies have already produced fuel cell electric vehicles. The progress in the production and manufacturing of fuel cell vehicles is attached to the cost associated with these vehicles. Since 2008 automotive fuel cell prices have fallen 70% thanks to technological progress and growing sales of fuel cell electric vehicles (FCEVs) [5].

Hydrogen has been successfully applied to heavy-duty vehicles such as buses, and in the last years, it has been introduced in a few trucks as it is shown in Table 2. One-fifth of the production of fuel cell vehicles are buses and medium-duty trucks. However, as hydrogen vehicles are fairly new on the market and still have a lot of room for improvement, the total number of FCEVs is still far below the estimated 11 million electric vehicles on the road today [5].

Electric or hydrogen vehicles are not the only innovations that can improve to minimize the emissions of the road transport sector, autonomous vehicles do as well. Automated driving systems (ADS) are already implemented in some vehicles on the market, and they are considered one of the best achievements of the sector. This could revolutionize the way people and freight move on-road by calculating and optimizing speed profile at any moment to minimize fuel consumption, [7]. This leads to an increase in productivity and profitability for freight road transport. ADS allows passenger cars to reduce 10% the fuel consumption but a significant decrease is noticed in freight road transport. Integration of automation, artificial intelligence, information, and communication accelerates, and the development of connected and automated vehicles (CAV) has become a collective goal in the industry [22, 23].

Many factors affect the profitability of different vehicle types; the operating range, payload, weight and volume of goods, charging infrastructure, utilization level, purchase cost, battery life, energy consumption, average speed, available routes, and logistics, which tip the balance in favour of one another type [23].

Table 2: Fuel cell electric trucks and semitrucks in the current and future market

Heavy duty vehicle model	Company	Date
Hyundai Xcient Fuel Cell	Hyundai	2020
Kenworth T680 FCEV	Kenworth/Toyota	2021
Hino Dutro light-duty FCET	Hino	2021
Hyzon class 8	Hyzon	2022
Hyzon Hymax series	Hyzon	2021
Hyzon Econic	Hyzon	2021
Hyzon Drayage	Hyzon	Unknown
Mercedes-Benz GenH2 Truck	Mercedes	2023
Nikola tre	Nikola	2023
Nikola two	Nikola	2024
Hino Profia FR1AWHG	Toyota/Hino	Unknown

Overall, diesel engines in HDVs will remain the main technology in the near future due to the existing infrastructure and lower costs, despite their high emissions, while battery electric HDVs technology and hydrogen fuel cell HDVs technology will be slowly developed to eliminate their barriers, including costs, infrastructure, and performance limitations, to penetrate the market [24].

1.2. Literature Survey

The main goal of this thesis is to minimize the energy and hydrogen consumption of a fuel cell electric truck by solving an optimal control problem and obtaining the trade-off consumption over trip time. Energy and hydrogen consumption depends on different factors such as the vehicle load, the elevation profile, traffic, weather, or speed and power distribution along the route. Some of them cannot be influenced by our actions but the speed and power distribution are parameters to control and optimize to reduce the consumption of the vehicle. This thesis presents a hierarchical optimization that splits the global optimal control problem into two sub-problems: optimal speed planning, and energy management control.

In recent years, it has been developed several technics and approaches to this problem. The strategy to solve optimal control problems for speed planning and energy management widely spread in scientific research is through the use of dynamic programming, to ensure global optimality to the optimal control problem [25]. Other reports solve the optimal control problem by using Pontryagin's minimum principle PMP as a benchmark, and the results are compared to a predictive controller model with a receding horizon approach, MPC [26]. Another strategy to solve the optimal control problems for electric vehicles instead of only using dynamic programming is by implementing firstly PMP to obtain the minimum operational modes and then solving the problem using dynamic programming with the new control grid [27]. This strategy decreases the computational time without a significant increment in energy consumption. Non-linear programming NLP, kinetic energy control KEC, estimated minimum principle EMP, or a mixed-integer quadratic program could be also used to solve this problem [28, 29, 30].

Implementation of optimal speed planning, energy management control, or both controls, depends on the number of energy sources of the vehicle. For vehicles with only one energy source such as battery electric vehicles or ICE vehicles is only necessary an optimal speed planning to minimize the energy or fuel consumption. On the other hand, if two energy sources are used in the vehicle, in hybrid vehicles or fuel cell electric vehicles, for instance, it is usually implemented an energy management control to optimize the power distribution between energy sources. In addition, the number of state and control variables depends on the complexity of the powertrain, therefore, on the type of vehicle. The powertrain of electric vehicles is simpler than ICE vehicles so the optimization for these vehicles contains fewer variables as well. The battery power is modelled as an equivalent electric circuit, with an ideal voltage source and an internal resistance in series, [31]. Hybrid electric vehicles consist of an ICE and an electric motor, so the model must introduce both systems. Finally, fuel cell electric vehicles use electric batteries and fuel cells as energy sources and this energy is applied to the electric motor to move the vehicle. The complexity of the optimal control increases with more variables in the model increasing computational time. Dynamic programming suffers from this computational burden if the number of variables increases, denoted as curse of dimensionality, so the number of state and control variables must be as lowest as possible.

The simplest speed planning model is implemented using only speed as a state variable for electric vehicles and speed and gear for internal combustion vehicles. In [32] is used dynamic programming to obtain the speed planning for a light diesel vehicle, in [33] for a heavy-duty vehicle, and in [34] for a battery electric HDV. In that work is provided a deep study of the influence of the topography. Slopes on the road increase fuel consumption and affect the optimal speed distribution to obtain the minimum consumption for a specific time. It is observed that before the top of the uphill, the vehicle increases the speed and then starts a coasting phase to optimize fuel consumption. More complex approaches to simulate real scenarios and calculate the speed profile to minimize fuel consumption are designed by adding normal traffic behaviour with stops or including driver comfort terms within the objective function [32, 27, 35].

Other reports only model the energy management, and the speed distribution is given. The state variables frequently used to accomplish the energy management control are the state of charge, SoC, and the rest of the variables depend on the type of vehicle, hybrid or fuel cell electric. In [36] the speed trajectory for a fuel cell electric light vehicle comes from adaptive online learning enhanced Markov velocity forecast approach, and the energy management is calculated using MPC. This energy management strategy is also used in [37] using a truck and including the effects of traffic lights as well as in [38], where it is optimized the fuel consumption and the work-life of the batteries of a fuel cell bus. Other different strategies to solve the energy management problem are fuzzy logic control (FLC) and operating mode control (OMC) [39]. Finally, it is very interesting the result comparison to optimize the fuel consumption and lifetime of the hydrogen fuel cells from a fuel cell electric vehicle using different strategies in real scenarios including the elevation profile of the road [40].

The combination of both optimal speed planning and energy management control lets us calculate the optimal speed and power distribution from the information on the road. This could be achieved in two different ways, either with a co-optimization or with a hierarchical optimization. Co-optimization uses only one optimal control problem to obtain the minimum fuel consumption, meanwhile, hierarchical optimization split the optimal control problem into two sub-problems: optimal speed planning and energy management control. In [41] the velocity optimization and energy management are solved in a co-optimization by using dynamic programming, and in [42] the speed trajectory is calculated first using dynamic programming and the energy management using an MPC under real-time conditions in a hierarchical optimization for a fuel cell electric bus. The benefits and drawbacks of using co-optimization or hierarchical optimization strategies are discussed in [43] and [44] where it is also included several methods to reduce computational time by replacing state variables by tuning terms in the objective function.

Many researchers have indicated that eco-driving techniques are effective to reduce fuel consumption, and they have been promoted with the slogan, ‘10 tips for fuel-conserving eco-driving’ [45]:

- 1) **Accelerate gently.**
- 2) **Keep your speed constant.**
- 3) **Slow down by decelerating.**
- 4) Limit the use of your air conditioner.
- 5) Do not idle your engine.
- 6) Do not warm up your engine before starting off.
- 7) Know your itinerary.
- 8) Check your tire pressure regularly.
- 9) **Reduce your load.**
- 10) Respect parking regulations.

Tips from 1) to 3) represent methods to influence the driver’s pattern on the road. Tips 4) – 6), 8), and 9) show methods to realize low-fuel consumption without changing the running pattern, item 7) is a method to reduce fuel consumption itself by reducing the vehicle mileage, and item 10) is equivalent to a method to realize fuel-efficient traffic flow. This master’s thesis will focus on the items from 1 to 3 which are related to the driving behaviour, and they will be included in the objective function of the optimal control problem. “Accelerate gently” can be included using the jerk term and “keep your speed constant” by a smooth term that penalizes sharp changes in the speed. However, as it will be discussed later, including a jerk term in the objective function is attached to add an interpolation in the programming code which leads to slower simulations, so only a smooth term is applied for this work. Also, tip number 9, “Reduce your load” is evaluated in this thesis simulating the truck for different admissible loads over time.

Another studio about minimizing the fuel consumption by the driving behaviour is a german eco-driving study including the tip “release gas pedal and keep coasting in the velocity range of good fuel-efficiency”, for a better fuel consumption, [46]. In the case of battery electric or fuel cell electric vehicles, during coasting it is used zero electrical power in the system. German eco-driving is related to the technique Pulse-and-Gliding (PnG) strategy which is also known to achieve better fuel economy in light traffic, like SAE Supermileage Competition [47]. Its basic idea is to run the engine at high power, store kinetic energy in vehicle inertia, and then coast down to a low speed only using that energy (while the engine is off or the system is not providing power to the motor) [48].

The experimental results reported that the fuel consumption rates of the Japanese and the German eco-driving improved by 11.6-15 % and 7.1-14 % respectively, compared to normal driving, [46]. In addition, data analysed for American Trucking Associations’ (ATA) Technology and Maintenance Council shows a 35 percent difference between the most and least efficient drivers. From this studio, they noticed that the reason for these differences was because the drivers use mainly the same the

technics discussed in the Japanese and German reports adding more value to these reports [49].

1.3. Contribution

This master's thesis aims to give a new insight into the minimization of energy and hydrogen consumption for a defined route, as well as provide an analysis of the trade-off between energy and hydrogen consumption and driving time. The chosen route is a highway of 70 km located in Austria where will be simulated the behaviour of a fuel cell electric truck. The elevation profile is considered for the optimization because for HDVs this produces a high impact on the resistive forces so it cannot be neglected in order to obtain a realistic fuel consumption and speed profile.

For this purpose, optimal speed planning and energy management control have been designed using dynamic programming. Simulations are based on the data of the route driven by the HDV as an input, and the route and vehicle constraints are imposed in the simulation model. The optimal control model calculates first the optimal speed and electrical motor power distribution along the route to minimize the energy of the system and then, these data are used as inputs for the energy management control to optimally distributes the use of hydrogen fuel cell and electric battery power to reduce the total hydrogen consumption.

Results from the optimal speed planning using exclusively dynamic programming are compared with the strategy formulated in [27], where Pontryagin's minimum principle is used to obtain the minimum number of operational modes to reduce the decision grid, and then, the optimal control problem is solved using dynamic programming. Once the strategy to solve the global optimization is chosen, different truck loads, elevation profiles, and the trade-off energy and hydrogen consumption over driving time are analysed. Both strategies avoid mechanical braking and provide similar energy consumption values. PMP reduces the computational time in the speed planning control but the speed and power profiles from a wide grid using dynamic programming are smoother and more realistic.

Another important analysis in the thesis is the study of how to reduce the ohmic losses and therefore, decrease the overheating of the batteries and increase their lifetime. To this end, a penalty is included for exceeding high motor power values and different objective functions are evaluated in the optimal speed planning and energy management control to compare their effects on the ohmic losses and the hydrogen consumption of the truck. Results of using power constraints and different objective functions achieve reductions of 25-30 % in ohmic losses with increments of 1-2 % in hydrogen consumption.

1.4. Outline

Section 2 explains the powertrain of the fuel cell electric truck, vehicle dynamics, driving cycles, and basic concepts of dynamic programming. Then, section 3 discusses how optimal speed planning and energy management control are implemented using dynamic programming, state and control variables, and constraints. Section 4 shows the results of the different scenarios and objective functions to end in section 5 with a summary of the main findings of the master's thesis.

2. Background

This section introduces the vehicle modelling, the route driven by the truck, and basic concepts of dynamic programming. The optimization and how it is implemented for the fuel cell electric truck is explained afterwards.

2.1. Vehicle Modelling

This work aims to simulate the optimal behaviour and consumption of a fuel cell electric truck on a real long trip. For this purpose, it is defined the architecture of the electric powertrain, vehicle dynamics, the battery and fuel cell system and parameters and constraints of the truck and the road.

2.1.1. Vehicle dynamics

The vehicle powertrain used in this thesis consists of an electric motor, a battery system, and hydrogen fuel cells. The battery system and the hydrogen fuel cells are the energy sources of power for the system. Combining two different energy sources increase vehicle range, provides higher power and allows regenerative braking charging the batteries. At the same time, the use of hydrogen fuel cells reduces battery degradation by reducing the use of high battery power values during the trip.

The electric motor and the fuel cell system are connected to an AC/DC and DC/DC power converters respectively to transmit the power, meanwhile, the battery system is directly connected without any power converted. A scheme of the architecture of the powertrain is shown in Figure 2.

One of the benefits of using an electric motor is the possibility to transmit energy from the wheels to the system to charge the batteries or to cover the vehicle's auxiliary losses, so total energy consumption is reduced. The electric motor is used as a regenerative motor during brakes providing energy to the system and charging the batteries until the regenerative power limit of the motor is reached. Above that limit, the motor is not able to transmit the power to the system and the power is converted into heat as standard mechanical braking.

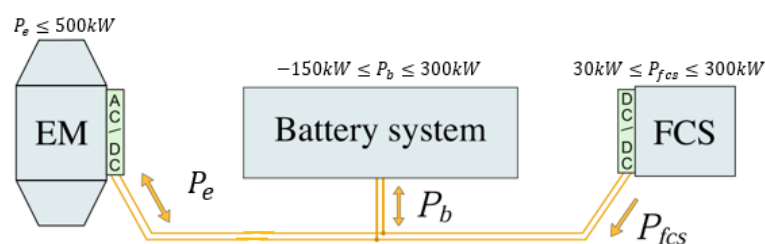


Figure 2: Powertrain of the fuel cell electric truck.

To determine the dynamics of the vehicle, the resistive forces acting on the fuel cell electric truck must be calculated for each moment of the trip. Resistive forces are split into three different forces; rolling resistance force, F_{roll} , grade resistance force, F_{slope} , and the air resistance or drag force, F_{drag} . These forces depend mainly on the speed of the truck, the slope of the road, and the vehicle mass.

F_{roll} is the force opposing the movement in the forward direction of the vehicle rolling on the road. Occurs due to the friction between the tires and the driving surface. It depends on the vehicle mass, the slope of the road, and the rolling resistance coefficient, c_r , which is influenced by the wheel design, rolling surface, or wheel dimension [50, 51]. F_{slope} or gradient forces must be considered driving on an uphill or downhill road. This force is positive for uphill and negative for downhill. The value of the gradient forces for high slopes plays a big role in the total resistance forces and in the optimal speed distribution. To minimize energy and hydrogen consumption it will be observed in the results how the vehicle switch between propulsion, coasting, and regenerative braking during changes in the slope of the road. This term depends on the vehicle mass as well as the rolling force [51]. F_{drag} opposes the vehicle's motion by the flow of the air around the vehicle. It increases with the speed and the front area of the vehicle. Other parameters that influence the aerodynamic drag forces are the drag coefficient, c_x , and the air density, ρ_{air} . Important to consider is that this force does not depend on the vehicle mass [51].

The equations of the resistance forces and the interaction between the vehicle and the road are depicted in Figure 3.

$$F_{roll} = m_v g c_r \cos\alpha \quad (1)$$

$$F_{slope} = m_v g \sin\alpha \quad (2)$$

$$F_{drag} = \frac{1}{2} A_v c_x \rho_{air} v^2 \quad (3)$$

$$F_{res} = F_{roll} + F_{slope} + F_{drag} \quad (4)$$

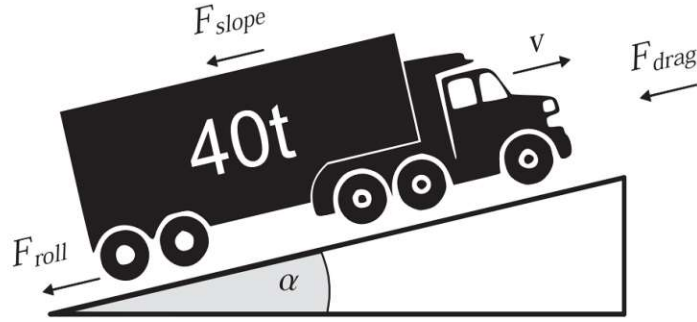


Figure 3: Representation of resistances forces on the truck. Source: [40]

Once the resistance forces of the heavy vehicle have been calculated, the power of the electric motor can be calculated. Firstly, the power at the wheels P_w is calculated as the sum of the resistance forces and the force needed to accelerate the vehicle.

$$P_w = (m_v \dot{v} + F_{res})v \quad (5)$$

The power from the electric motor to the wheels is affected by the power losses of the electric motor itself, the power converters, and other losses of the drivetrain components. These terms are represented and considered in the model by the total efficiency, η_T . The relationship between the electric motor power and the power at the wheels depends on the direction of power transmission as the electric motor could operate as a propulsion motor (power from the motor to the wheels) or as a regenerative motor (power from the wheels to the motor). This concept is included in the equations with the sign of the power at the wheels in the powder of the total efficiency, equation (6).

$$P_e = P_w \eta_T^{-sgn(P_w)} \quad (6)$$

2.1.2. Fuel cell system.

The fuel system of the fuel cell electric truck studied in this thesis consists of multiple stacks and auxiliary components. Stacks are used to provide the required voltage and power to the system by connections of fuel cells in series and parallel.

The fuel cell power provided by the stacks depends on many different factors of the cells such as the current, temperature, relative humidity, and partial pressure of the reactants. The value of these parameters should be calculated or known to predict an accurate behaviour and dynamics of the cells. However, in this thesis, all terms are considered constant using the auxiliary losses, so the fuel cell power provided to the

system is the difference between the fuel cell from the stack and the auxiliary losses. In addition, the DC/DC converter is considered ideal and the losses from it are neglected.

$$P_{fcs} = P_{fcs,stack} - P_{fcs,aux} \quad (7)$$

To calculate the hydrogen consumption of the vehicle, specific hydrogen consumption, μ_{H_2} , hydrogen lower heating value, LHV_{H_2} , fuel cell system efficiency, η_{fcs} and fuel cell power are used. LHV_{H_2} is considered constant whereas fuel cell system efficiency depends on the fuel cell power as you can observe in Figure 4.

$$\mu_{H_2} = (\eta_{fcs} LHV_{H_2})^{-1} \quad (8)$$

$$\dot{m}_{H_2} = \mu_{H_2} P_{fcs} \quad (9)$$

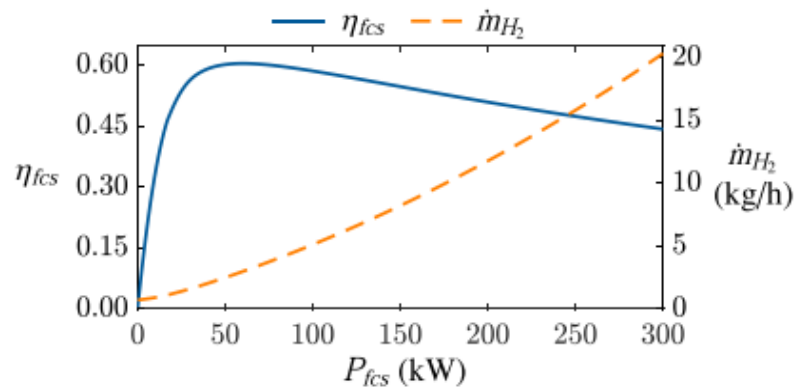


Figure 4: Fuel cell system efficiency and hydrogen fuel cell mass respect to the fuel cell power. Source: [40]

2.1.3. Battery system

The battery system is represented by an open-circuit voltage source connected in series with an internal resistor R_{int} in Figure 5. The power supplied by the battery to the system P_b is calculated from the current flowing in the circuit and the total circuit voltage by Kirchhoff's law. Battery power will be positive while the battery system is discharging and negative when the battery is charging, e.g., during regenerative braking.

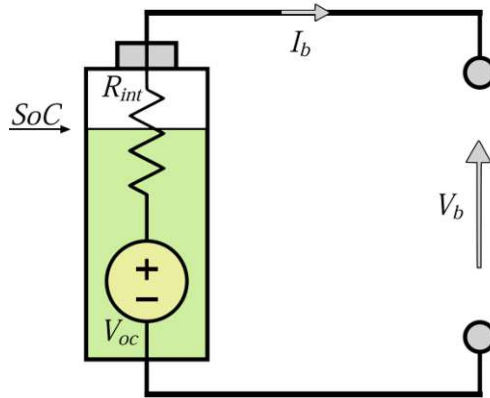


Figure 5: Scheme of the battery system. Source: [40]

$$P_b = V_b I_b = (V_{oc} - R_{int} I_b) I_b \quad (10)$$

The battery system is actually composed of a battery cell pack connected in series and parallel, Figure 6. The fuel cell electric truck simulated in this thesis is constituted of 110 and 50 batteries in series and parallel respectively, (N_{serie} , $N_{parallel}$). Ohm's law is used to calculate the total internal resistance and open-circuit voltage of the battery system.

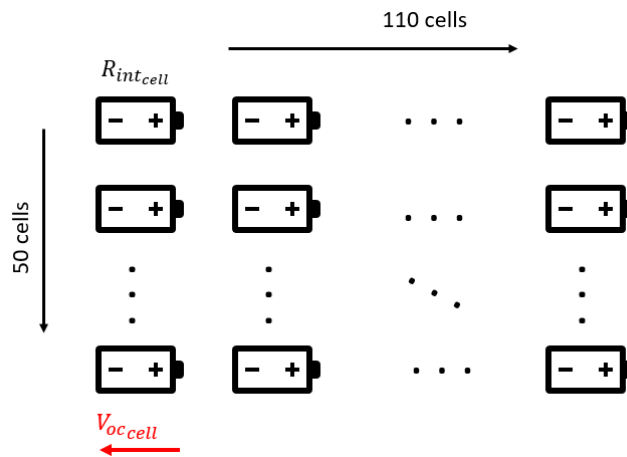


Figure 6: Representation of the battery pack in the vehicle.

$$R_{int_{serie}} = N_{serie} R_{int_{cell}} \quad (11)$$

$$R_{int} = \frac{1}{\frac{N_{parallel}}{R_{int_{serie}}}} \quad (12)$$

$$V_{oc} = N_{serie} V_{oc_{cell}} \quad (13)$$

In addition, open-circuit voltage and the internal resistance values of each cell depend on the state of charge, SoC. Open-circuit voltage value increases with increasing the SoC, but the internal resistance of the cells decreases with it. Dynamics and values of the internal resistances and open circuit voltage are represented in Figure 7 and Figure 8. The model proposed in the thesis considers that all the cells are charged and discharged at the same time, so the SoC is the same for all of them as well as the internal resistance and the open-circuit voltage.

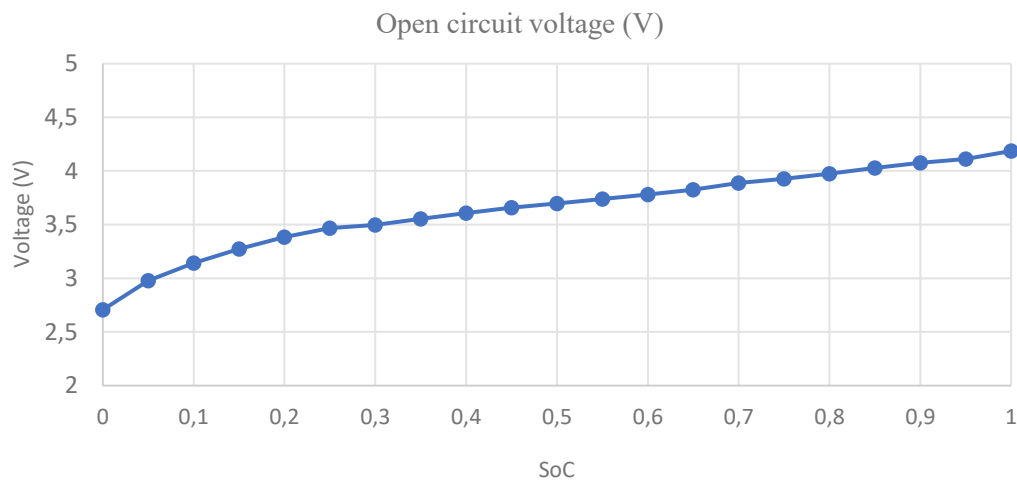


Figure 7: Open Circuit Voltage over SoC

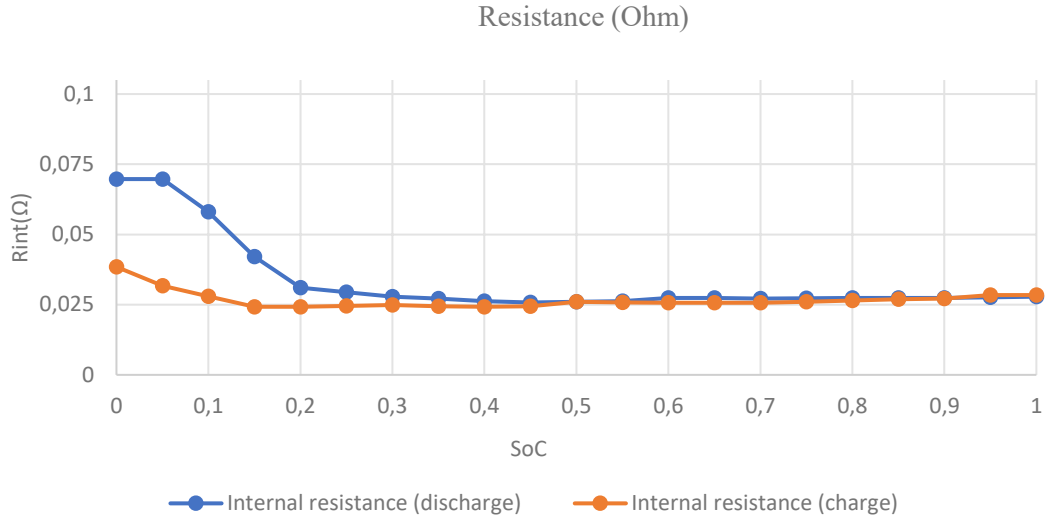


Figure 8: Representation of the resistance over SoC for both charge and discharge operation modes

From the battery power equation, it is obtained the battery current to the system expressed as a function of the power, internal resistance, and open-circuit voltage following the equation (14).

$$I_b = \frac{V_{oc} - \sqrt{V_{oc}^2 - 4P_b R_{int}}}{2 R_{int}} \quad (14)$$

The battery current, I_b , is the equivalent current delivered from the battery pack to the system. Using this current and the equivalent internal resistance of the battery pack allows us to calculate the ohmic power. The ohmic power value P_Ω is converted into heat deteriorating the batteries, so this term is used to analyse the batteries' behaviour. Therefore, minimizing the ohmic power leads to improvements in battery lifetime which could be achieved in the model by implementing motor power constraints or modifying the cost function.

$$P_\Omega = R_{int} I_b^2 \quad (15)$$

The state of charge is calculated as the rate between the current and nominal charge, Q and Q_{nom} . The initial and final SoC of the model will be assigned beforehand to the simulation so the main parameter that must be calculated is the Δ SoC to know the SoC increments and calculate the following values. This is obtained by the rate between the current and the nominal charge, so the dynamics of the state of charge are defined as a function of the battery power and the actual SoC.

$$SoC = \frac{Q}{Q_{nom}} \quad (16)$$

$$S\dot{o}C = \frac{\dot{Q}}{Q_{nom}} = -\frac{I_b}{Q_{nom}} = -\frac{V_{oc} - \sqrt{V_{oc}^2 - 4P_b R_{int}}}{2 R_{int} Q_{nom}} \quad (17)$$

Finally, once it has been explained the battery and the fuel system, the electric motor power can be redefined as the sum of both terms.

$$P_e = P_b + P_{fcs} \quad (18)$$

2.1.4. Parameters and constraints of the vehicle

The model parameters and the constraints of the vehicle are summarized in Table 3. Vehicle constraints are applied to the electric motor power, fuel cell power, battery power, and state of charge. The electric motor power is limited by the maximum power that it can deliver to the system. Fuel cell power presents a lower bound, $P_{fcs, idle}$ and an upper bound $P_{fcs, nom}$. Fuel cell power lower bound is used to force idle operation which limits the degradation by preventing fuel cell shutdowns and low power. Battery power is constrained to the maximum charge limit $P_{b, ch}$ and discharge limit $P_{b, dis}$. The state of charge is also constrained to prevent the degradation of the batteries. Higher or lower values of the SoC of the battery affect increasing battery degradation. To avoid this, it is implemented SoC limit range from 0.5 to 0.8.

The vehicle load is considered 35 tonnes by default, but it will be changed in some simulations to observe the difference in consumption for different loads. Note that other parameters such as the internal resistance and the open-circuit voltage are also defined in Table 3 to give an idea of the general values, but they are not constant during the simulations.

Parameter	Symbol	Value	Unit
Vehicle mass	m	35000	kg
Gravitational acceleration	g	9.81	m/s ²
Rolling friction coefficient	c_r	0.01	-
Vehicle frontal area	A_v	8	m ²
Drag coefficient	c_x	0.35	-
Air density	ρ_{air}	1.2	kg/m ³
Total efficiency	η_T	0.87	-
Hydrogen lower heating value	LHV_{H_2}	120	MJ/kg
Open-circuit voltage	V_{oc}	380	V
Internal resistance	R_{int}	0.05	Ω
Nominal charge	Q_{nom}	200	Ah
Idle power	$P_{fcs, idle}$	30	kW
Nominal fuel cell power	$P_{fcs, nom}$	300	kW
Max charging power	$P_{b, ch}$	- 150	kW
Max discharging power	$P_{b, dis}$	300	kW
Nominal motor power	$P_{e, nom}$	500	kW
Min state of charge	SoC_{min}	0.5	-
Max state of charge	SoC_{max}	0.8	-

Table 3: Parameters of the fuel cell electric truck

2.2. Driving cycles

One of the contributions of the thesis to the feasibility and study of fuel cell electric trucks is the simulation of a real long driving cycle. In this way, it is possible to know more precisely how the truck will behave in realistic scenarios such as long uphill and downhill.

For the study of the consumption and trade-off consumption over trip time, it is simulated a motorway of approximately 70 km from Austria with high elevation and slopes on the road. This allows us to observe and analyse different consumption parameters over a wide range of time. Many studies either do not perform simulations on this type of road, or neglect the resistive forces associated with the elevation of the road, so more insights and documentation about optimal speed planning and energy management control for HDV are needed. The route is defined with the elevation profile in a very complete way, although for possible future studies we could also consider the road in 3 dimensions evaluating the influence of the curves in the road and how the truck should behave to minimize the consumption in that new scenario, which is outside of the scope of this thesis.

The fuel cell electric truck modelled in this master's thesis was monitored to obtain the real driving data and to perform simulations in a real route. The speed profile is filtered to remove sharp changes in the speed due to traffic or external factors of the road that are not considered in the simulation model. The upper speed limit for the simulations is the same as the real driving speed data, although the minimum speed

limit was set lower than the real speed data to compare results with a wider range of speed options. Figure 9 shows the elevation and speed profile monitored from the truck.

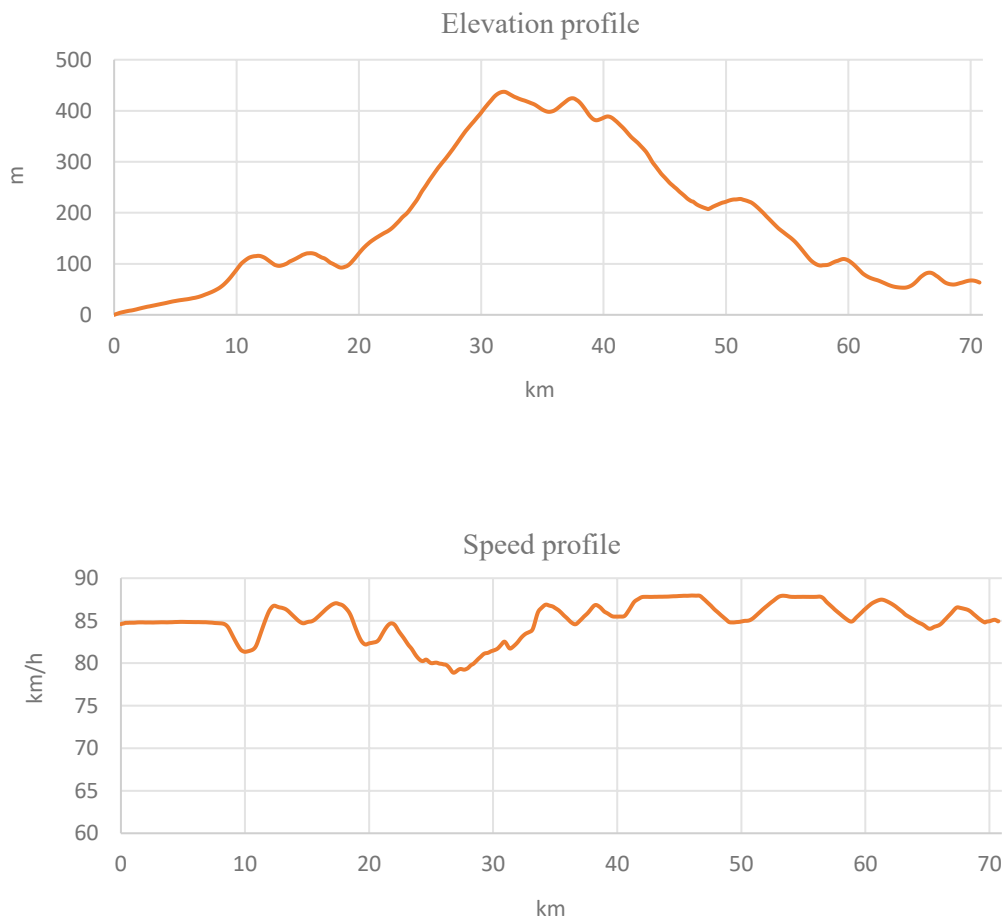


Figure 9: Driving cycle (Uphill) from real data.

Most of the simulations are done with the real route described above, however, to compare the difference in consumption between routes with different elevation profiles it was chosen another flatter section also monitored by the truck, Figure 10. Both sections are modified to match initial and final elevation of the elevation profile. This is done since an increase in the elevation at the end of the road with respect to the starting point implies an increase in energy and hydrogen consumption.

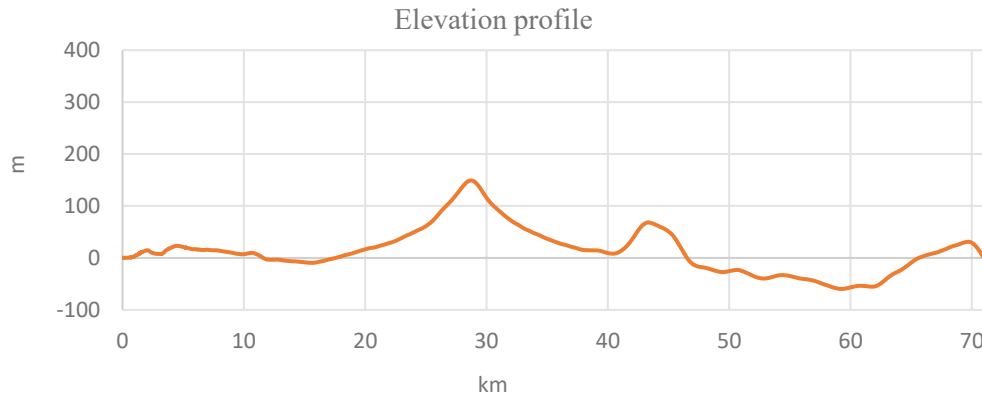


Figure 10: Driving cycle (Flat cycle) adjusted start and end elevation to zero

2.3. Dynamic programming

To solve the optimal control problem, it is chosen the dynamic programming technique based on the Bellman's principle. Dynamic programming is a method to solve optimal control problems which aim to minimize an objective function ensuring the global optimality. The objective function must be well defined, and it could include different terms such as fuel consumption, trip time, driver comfort, or ohmic losses.

2.3.1. Dynamic programming formulation

Dynamic programming breaks the global optimization problem into small and simple steps over time or space. In this thesis, the problem is formulated as a finite horizon optimal control problem. To split the optimal control problem, the time horizon is denoted by the integer N , so the control problem will be solved for $k = 0, 1, \dots, N$, time steps.

Optimal control problems are solved by the proper selection of the state and control or decision variables. By definition, state variables in a problem are those that a decision-maker takes as given when making choices in each period, but future values are either determined by current choices or unknown at the current time. Decision or control variables are the variables that can be tuned in the system to interact and modify the future state variables. The evolution of the state is subject to control and disturbances, equation (19). The definition of a problem entails selecting an appropriate state, characterizing the available measurements, the process, and measurement disturbances, as well as establishing which controls or decisions are accessible and how they affect the system's dynamics and measurements.

From literature and several reports, it is established to use for optimal control vehicle problems the speed as a state variable, x_k , power, torque, and gear, as control variables, μ_k , and slope of the road as disturbances, θ_k , [52, 36].

$$X_{k+1} = f(X_k, U_k, \theta_k) \quad (19)$$

Optimal control problems calculate the minimum of the objective function or cost function by choosing the appropriate control policy $\pi = \{\mu_1, \dots, \mu_{N-1}\}$ that leads the system to next states. The cost associated for each stage is called stage cost, $c_k(x_k, \mu_k)$, from $0 \leq k \leq N - 1$, and at the last period the cost function incurred the terminal cost, $c_N(x_N)$. The cost function is considered to be additive over time with an expected total cost $J_0(x_0, \pi)$, as it is shown in equation (20) [52].

$$J_0(x_0, \pi) = E \left[c_N(x_N) + \sum_{k=0}^{N-1} c_k(x_k, \mu_k) \right] \quad (20)$$

The optimal control policy, π^* , is the sequence of control variables in the set of admissible policies Π for each stage that minimize the cost function from the initial state to the final state. The minimization leads to the optimal cost function or optimal value function.

$$J_0^*(x_0) = J_0(x_0, \pi^*) = \min_{\pi \in \Pi} J_0(x_0, \pi) \quad (21)$$

Dynamic programming is based on the principle of optimality defined by Richard Bellman. This principle says the following: Assume that exists an optimal policy $\pi^* = \{\mu_0^*, \mu_1^*, \dots, \mu_{N-1}^*\}$ for an optimal control problem which reaches the state x_i at time i . Consider a sub-problem from the state x_i at time i until time horizon N , then the truncated policy $\pi^i = \{\mu_i^*, \dots, \mu_{N-1}^*\}$ must minimize the optimal subproblem [52].

$$J_i(x_i, \pi^i) = \min_{\pi^i = \{\mu_i^*, \dots, \mu_{N-1}^*\}} E \left[c_N(x_N) + \sum_{k=i}^{N-1} c_k(x_k, \mu_k) \right] \quad (22)$$

Dynamic programming (DP) algorithm computes backwards in time, solving successively all the tail subproblems. Backward computation solves from the tail

subproblem at time N to the initial time, therefore, the cost function at time N is trivial since it does not involve any control choice.

$$J_N^*(x_N) = c_N(x_N). \quad (23)$$

For the computation of the rest of the subproblems at time k , the optimal function $J_k^*(x_k)$ is solved from the previous tail optimal function step value $J_{k+1}^*(x_{k+1})$.

$$J_k^*(x_k) = \min_{U_k(x_k)} E [c_k(x_k, \mu_k) + J_{k+1}^*(x_{k+1})] \quad (24)$$

The backward subproblem solution store a data-table or matrix of the optimal control versus the states for each time step. Then, it is rebuilt the optimal control from the initial state by using the mapping stored at each iteration for $k = [0, 1, \dots, N - 1]$.

$$U_k^* = \mu^*(X_k) \quad (25)$$

$$x_{k+1} = f(X_k, U_k^*) \quad (26)$$

2.3.2. Curse of dimensionality

The traditional term, *curse of dimensionality*, was denoted by Bellman in reference to the computational time and storage requirements to solve dynamic programming problems of several state variables. Although, it is also present in any control theory approach where a set of equations are numerically solved, (one equation for each state variable) [52]. The curse is total number of states that limit the application of the technique. The number of states is not only the number of state variables, but the product of the number of states for each state variable. This parameter determines the storage and the computational time to solve the dynamic model.

It is one of the biggest issues of using dynamic programming to solve an optimal control problem. Increasing the number of state variables or control variables increases exponentially the volume of the space which leads to an increment in the level of complexity and computational burden. The optimal value function for all the stages, states and decision alternatives must be stored and calculated, so if the states are not properly chosen it could exceed the available memory or take a very long time to operate it. [53]

The issue of computational complexity must be mitigated by minimizing the number of variables and by using strategies such as the implementation of tuning

parameters to replace state variables or the use of the synthesis of Pontryagin's minimum principle previous to dynamic programming to reduce the control grid size.

3. Optimal Speed Planning and Energy Management

This section seeks to give a complete understanding of how the optimal control problem is solved. As a hierarchical optimization is used, the cost function of the optimal speed planning and the energy management control are presented as well as their respective objective functions using dynamic programming. In addition, the synthesis of Pontryagin's minimum principle is introduced to solve the optimal speed planning which will be compared with the previous strategy in the results section.

3.1. Optimization

The main purpose of this thesis is to minimize the energy and hydrogen consumption of a fuel cell electric truck, and to analyse the trade-off consumption over trip time. It is proposed a hierarchical optimization, hence, the optimal control problem is broken into two sub-problems, optimal speed planning and energy management. From the speed planning is obtained the speed and power distribution to optimize the global energy consumption of the electric powertrain. After that, these results are used as inputs in the energy management control to obtain the optimal split between the fuel cell power and the battery power of the truck to minimize hydrogen consumption.

A scheme of this hierarchal model is shown in Figure 11.

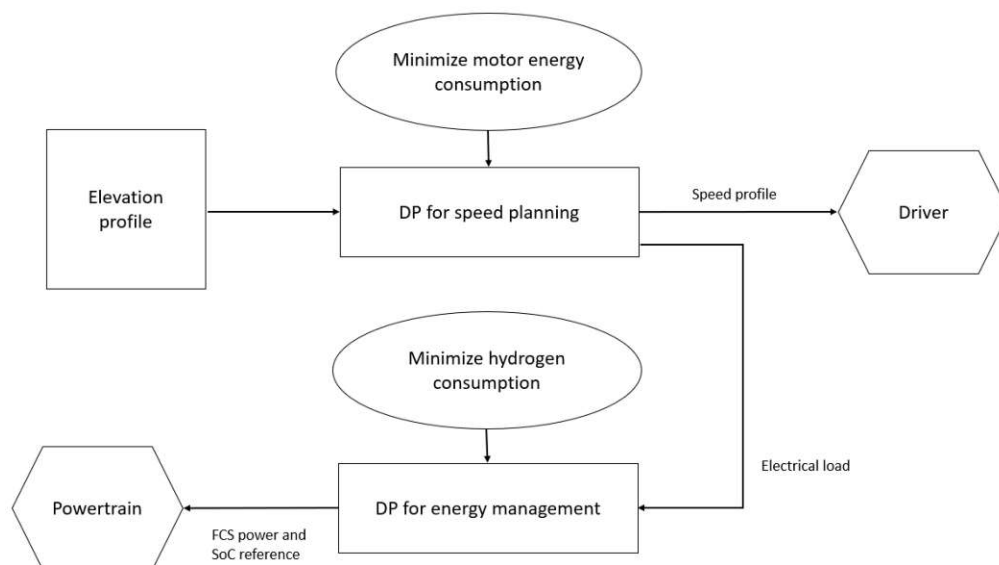


Figure 11: Scheme of the methodology used for the optimal speed planning and energy management

3.1.1. Cost function optimal speed planning

In this section are presented the equations and the cost functions of the optimal speed planning control to minimize the energy consumption for a specific time.

The total energy consumption for a trip is defined as the integral of the power over time, equation (27). Equation (28) presents the simplest cost function to minimize the energy consumption of the route.

$$E_T = \int_0^{t_f} P_e dt \quad (27)$$

$$J_{sp} = \min \int_0^{t_f} P_e dt \quad (28)$$

This equation only provides the minimum energy consumption, but it does not contain any time constraint or time tuning factor to determine a specific trip time. Because of this, the optimization is solved by increasing the trip time as much as possible since the lower the speed, the lower the energy consumption. To obtain the trade-off energy consumption over trip time or simulate the energy consumption for a specific trip time it is needed to include the time term in the equation.

To determine the time for the route could be done by two different strategies. The first strategy is adding the time as another state variable and defining a term cost to fulfil this time requirement. However, as it was explained in previous sections, if one state or decision variable is added to solve the problem by dynamic programming, the computational time increases exponentially, so this option should be avoided. The second strategy consists of including a tuning parameter associated with a weighting factor in the cost function. This factor penalizes the trip time, therefore, to obtain shorter or longer trip times it is only needed to modify the value of the weighting factor.

After adding the weighting factor, the cost function looks like this:

$$J_{SP} = \min \int_0^{t_f} P_e + \lambda_t dt \quad (29)$$

At this point, the total energy consumption and the cost function in the time domain are formulated, but for the optimization, it is needed to formulate the optimal control problem using the space domain. The input is the elevation profile of the route, and the time of the trip is calculated once the speed is determined for each space step to minimize energy consumption.

The following equations represent how the time domain is converted into space domain to optimize the model by dynamic programming.

$$dt = \frac{ds}{v} \quad (30)$$

$$P_e = F_e v \quad (31)$$

$$J_{SP} = \min \int_0^{s_f} (F_e(x, u) + \lambda_t \frac{1}{v}) ds \quad (32)$$

This raw cost function allows us to obtain the speed planning for different times, but it does not include other terms to be considered as the maximum regenerative braking of the fuel cell electric truck, mechanical braking, and driver comfort. One of the benefits of electric vehicles is regenerative braking. It allows the motor to transmit the power from the wheels to the system (negative power) when the vehicle brakes or drives on negative slopes (downhill). However, this regenerative braking is limited by the battery pack of the heavy-duty truck to -120 kW. Below this electric motor power, the batteries are not able to absorb more power from the brake and it is converted to heat. Mechanical braking must be included in the cost function to penalize the power below that limit. To implement that, it is used a power factor (ψ) which penalizes the cost function with the value associated with this mechanical braking as it is shown in the next equations.

$$\psi = \begin{cases} \frac{P_{reg}^{min} - P_e}{v}, & P_e < P_{reg}^{min} \\ 0, & P_e \geq P_{reg}^{min} \end{cases} \quad (33)$$

$$J_{SP} = \min \int_0^{s_f} (F_e(x, u) + \lambda_t \frac{1}{v} + \psi(x, u)) ds \quad (34)$$

Finally, the last term to include in the objective function is the smooth term (ϑ) to improve driver comfort and increase the sections of steady speed. By the weighting factor (λ_{smooth}) associated with this term, it is penalized sharp changes in the speed and avoided oscillations which benefit the vehicle fuel consumption. It also provides a more realistic speed profile to be followed by the driver. Examples and effects of this term are shown in the results chapter.

$$\vartheta = (v_k - v_{k-1})^2 \quad (35)$$

Then, the final objective function, over the space domain is defined with four terms: electric motor force, time term, mechanical braking term, and smooth term, equation (36). This objective function is solved by dynamic programming with the speed as the state variable and electric motor power as the control variable.

$$J_{SP} = \min \int_0^{s_f} (F_e(x, u) + \lambda_t \frac{1}{v} + \lambda_{smooth} \vartheta(x) + \psi(x, u)) ds \quad (36)$$

$$x = v \quad (37)$$

$$\frac{dx}{ds} = \frac{\frac{F_e(x, u)}{\eta^{-sgn(P_w(u))}} - F_{res}(x)}{m_v x} \quad (38)$$

$$u = P_e \quad (39)$$

3.1.2. Cost function energy management

Energy management uses the data provided by optimal speed planning to minimize hydrogen consumption. In chapter 2 is shown the calculation of the hydrogen consumption for the fuel cell electric truck, equation (9), so in this section, this equation is applied in the objective function. In this case, the cost function could be done either using space or time domain, because we have already the speed and elevation profile for each step. It was decided to continue using the space domain in the cost function for a better consistency of the equations.

The cost function for the energy management is defined as follows by using SoC as the state variable and the fuel cell power as the input variable:

$$J_{EM} = \min \int_0^{s_f} \left(\frac{\dot{m}_{H_2}(u)}{v} \right) ds \quad (40)$$

$$x = SoC \quad (41)$$

$$\frac{dx}{ds} = \frac{V_{oc}(x) - \sqrt{V_{oc}^2(x) - 4P_b(u)R_{int}(x)}}{2 R_{int}(x)Q_{nom} v} \quad (42)$$

$$u = P_{fcs} \quad (43)$$

This objective function does not entirely define the problem. It is still needed to include constraints on the speed and electric motor power in the optimal speed planning as well as constraints for the fuel cell power, battery power, and SoC in the energy management control to get a more realistic behaviour of the simulations of the vehicle.

3.1.3. Constraints in the optimization

Constraints in optimal speed planning are based on the speed and the electric motor power. Speed limits are based on a real driving scenario using data from the trucks on the road. The lower speed limit from the real heavy-duty vehicle for this route was reported at 19 *m/s* which is still high for the constraints in the electric motor power implemented in the model or to analyse the trade-off consumption over trip time for a wide range of time values. Therefore, it was decided to reduce this limit to 15 *m/s* to observe when the optimization actually reaches that limit and to obtain a better curve of the trade-off consumption over trip time.

Speed limits are included in the optimization as hard constraints as well as maximum motor power (500 kW). In addition, initial and final state variable values (speed of the vehicle) must be defined before solving the control problem by dynamic programming. To ensure that the final state value is reached at the end of the simulation the cost associated with that state in the last stage is set to 0 and the rest are set to a high-cost value to force that the minimum cost path contains it.

$$v_o = v_f = 23.5 \frac{m}{s} \quad (44)$$

Regarding the motor power constraints, this optimization implements soft power constraints from $0.5P_{e_{max}}$ to reduce the use of high values of motor power which detracts the battery behaviour in terms of ohmic losses. These soft constraints allow the optimization to use high motor power if it is necessary but avoid them if it is not. High vehicle loads, slopes on the road, or short trip times force the vehicle on some occasions to use high electric motor powers to overcome these situations.

Energy management control uses hard constraints for fuel cell power, battery power, and soft constraints for the SoC. As well as in the optimal speed planning,

initial and final state values of the SoC must be included in the formulation to solve the optimal control problem.

$$SoC_O = SoC_F = 0.65 \quad (45)$$

Summary of constraints implemented in the optimization are shown in the following equations:

$$v(s) \in [v_{min}, v_{max}] \quad (46)$$

$$P_e(s) \leq P_{e_{max}} \quad (47)$$

$$P_{fcs}(s) \in [P_{fcs_{min}}, P_{fcs_{max}}] \quad (48)$$

$$P_b(s) \in [P_{b_{ch}}, P_{b_{dis}}] \quad (49)$$

$$SoC(s) \in [SoC_{min}, SoC_{max}] \quad (50)$$

$$v(s_0) = v_0 \quad (51)$$

$$v(s_f) = v_f \quad (52)$$

$$SoC(s_0) = SoC_0 \quad (53)$$

3.1.4. Discretization of dynamic programming variables

The discretization of dynamic programming variables is essential for a good balance between energy or hydrogen consumption and computational time. These two parameters are the most important at the time of solving the optimization by dynamic programming. Increasing the grid size of the decision or state variables lead to a more accurate control, but at the same time, it is detrimental to the computational time as the optimization must perform more operations on each stage. Therefore, it

must be analysed the influence and the effect of using different grid sizes in the dynamic programming model for a good balance.

To analyse the data, the route is simulated with the same trip times using different input and decision grid sizes. Over the optimal grid, the energy or hydrogen consumption keeps the same value and only increases computational time, so it is critical to find the optimum values to reduce the computational time as much as possible without a considerable increment in the consumption. In addition, to design and choose a proper grid size, it must be observed the speed, power, and acceleration profiles do not present sharp changes and fluctuations. Optimal grid sizes for some terms are obtained from literature and others are chosen following the commented criteria.

Based on that, the discretization of the dynamic programming variables was chosen as follows:

Table 4: Discretization of dynamic programming variables

State	Symbol	Value	Unit
Velocity	Δv	0.1	m/s
Distance	Δs	100	m
Electric Motor Power	ΔP_e	2.82	kW
Fuel Cell Power	ΔP_{fcs}	1.5	kW
SoC	ΔSoC	0.005	-

3.2. Strategies to solve the optimization

In this section, it will be analysed two different strategies to solve the optimal control problem. Both strategies use dynamic programming to solve the optimal control problem, but the second one applies the synthesis of Pontryagin's minimum principle from the literature [43, 27] to reduce the grid size and decision variables to only 5 operational modes, and after that, the problem is solved by dynamic programming as usual. Pontryagin's minimum principle before solving the optimization by dynamic programming leads to benefits in computational time.

However, as you can see from the results, this method does not provide as accurate a speed and power profile as using a wide input grid.

3.2.1. Solve optimization problem by using directly dynamic programming

The most popular method to solve the optimal control problem is by using dynamic programming according to scientific reports. As it was explained in the background section, dynamic programming provides a global solution to the problem by the split of the global problem into subproblems and solving each of them. To use dynamic programming, the cost function must be reformulated as well as the cost terms as the sum of each stage. The following equations represent the optimal speed planning by dynamic programming formulation:

$$J_{SP} = \min_{(u_k)} \sum_{k=1}^N \left(F_e(x(k), u(k)) + \lambda_t \frac{1}{x(k)} + \lambda_{sm} \vartheta(k) + \psi(k) \right) \Delta s \quad (54)$$

$$x(k) = v(k) \quad (55)$$

$$acc(k) = \frac{\frac{F_e(x(k), u(k))}{\eta^{-sgn(P_w(u(k)))}} - F_{res}(x(k))}{m_v} \quad (56)$$

$$x(k+1) = \sqrt{x(k)^2 + 2acc(k)\Delta s} \quad (57)$$

$$u(k) = P_e(k) \quad (58)$$

Energy management control must also be converted to the corresponding dynamic programming nomenclature as the optimal speed planning to solve the optimal control problem.

$$J_{EM} = \min \sum_{k=1}^N \left(\frac{m_{H_2}(u(k))}{v(k)} \right) \Delta s \quad (59)$$

$$x(k) = SoC(k) \quad (60)$$

$$\Delta SoC(k) = \frac{V_{oc}(k) - \sqrt{V_{oc}^2(k) - 4P_b(k)R_{int}(k)}}{2 R_{int}(k)Q_{nom} v(k)} \Delta s \quad (61)$$

$$SoC(k + 1) = SoC(k) + \Delta SoC(k) \quad (62)$$

$$u(k) = P_{fcs}(k) \quad (63)$$

3.2.2. Solve optimization problem by using the synthesis of Pontryagin's minimum principle

As it is explained in previous sections, the discretization of the variables is crucial for the feasibility of the use of dynamic programming and to reduce computational time. From this idea, it was proposed to adapt the synthesis of Pontryagin's minimum principle from the literature to the optimal speed planning used in this thesis [27, 43]. This should reduce the computational time of the dynamic programming by simplifying the input grid to only 5 operational modes (full propulsion, coasting, full regenerative braking, full braking, and cruising). After defining these operational modes, the problem is solved by using dynamic programming as in the previous strategy.

This concept is implemented in the model to compare results for both strategies and evaluate their benefits and drawbacks. Note that in order to calculate the 5 operational modes, it is not included the driver comfort term in the objective function, but the rest of the terms, dynamic equations, and state variables remain the same. Information about how these 5 operational modes are calculated is included in the appendix.

4. Results

After defining the objective functions and the grid using dynamic programming, several simulations are performed to obtain the trade-off energy and hydrogen consumption over time for different scenarios. First, it is presented the results from the optimal speed planning to observe in detail the speed and power distribution along the route, and then, the energy management control is introduced to show the results of the global control problem.

4.1. Optimal speed planning overview

The first part of the global optimal control consists of calculating the optimal distribution of speed and power profiles to minimize the total energy consumption of the fuel cell electric truck, denoted as optimal speed planning. As it was mentioned in previous chapters, to simulate and solve the optimization, all parameters such as the grid size of the state and control variables, the objective function, and constraints must be well defined.

Power and speed constraints are implemented in this simulation as well as penalties related to mechanical braking and motor power limits to obtain realistic results. The optimal speed planning overview is done without implementing soft power constraints, although in the following section, the results are compared to the use of soft power constraints. Based on that, further simulations are performed by implementing these constraints. The vehicle load used for this simulation is 35 tonnes since this is the most often vehicle load used for the fuel cell electric truck. The trip time is adjusted by the weight time tuning term, which allow us to compare the consumption in different scenarios for a similar time as well as obtain the trade-off consumption over trip time by modifying its value. From Figure 12 is observed the overview of the speed planning results.

Regarding the optimal speed profile to minimize the energy consumption of the electric motor for a given time, it is observed that is not used the whole speed range within the speed limits available for the fuel cell electric truck. For a standard trip time in a realistic scenario, as the proposed simulation, the upper-speed limit is reached in several sections of the route, but the lower-speed limit is not used, being 65 km/h, the minimum speed driven by the truck. The speed profile is greatly influenced by the elevation profile and the slopes on the road. From the start of the route up to 30 km the overall slope of the elevation profile is positive and the fuel cell electric truck drives at constant speed. It only suffers small deviations in the speed during changes in the sign of the slope. On the other hand, along the downhill from 38 km to 70 km, the vehicle accelerates and decelerates more aggressively because it uses regenerative braking to reduce the total energy consumption of the motor and to not exceed the upper-speed limit. When the truck drives a small uphill, it slows down, and after the top of the hill is reached it starts to accelerate again. The

acceleration from the simulation is also within realistic limits ($\pm 1.5m/s^2$). It presents several sections with constants values equal to zero because of the smooth term which improves the drive comfort and fuel consumption.

The electrical motor power plot shows the power distribution which will be split into the battery and the fuel cell system. Along the sections with high slopes, the electric motor employs high electrical power to keep constant the speed. This is shown from 20 to 30 km where the electrical power increases to almost reach their maximum, although it never exceeds 500kW. The minimum value of the regenerative power provided by the fuel cell and battery models is represented with the green line at -120 kW. In any section of the road the electrical motor power is below the regenerative braking limit, which means that mechanical braking is completely avoided. These results were expected from the optimization because the energy from regenerative braking is considered as negative energy in the system able to use in other sections and to charge the battery or electrical components of the vehicle, but the energy from the mechanical braking is converted only into heat, so it is not beneficial to the system. Mechanical braking is only used when high deceleration is needed to keep from exceeding the upper-speed limit during negative slopes of the highway, which is not the case.

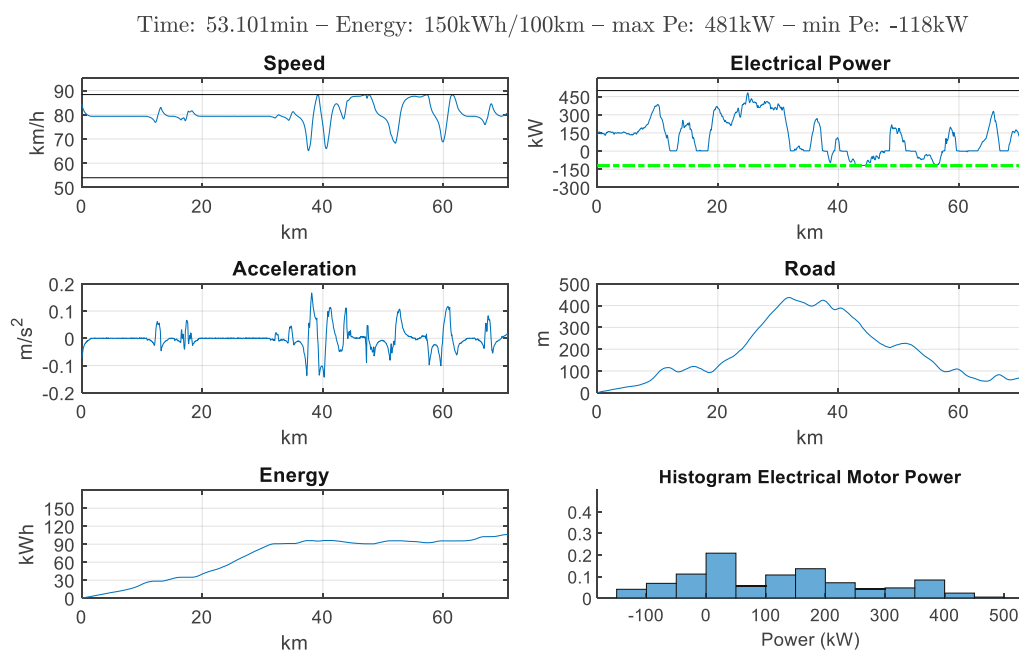


Figure 12: : Overview of the optimal speed planning results. Speed and power hard constraints are show by a black line and power linear constraints by a dash-line. Regenerative power limit is also shown in the electric motor power plot by the green dash-line.

Finally, the histogram shown in the speed planning overview gives us more information in a visual way about how the electric motor power of the truck is distributed along the road. From this histogram, as well as from the electric motor power plot is observed that it is completely avoided the use of mechanical braking,

and it is used frequently coasting to improve and reduce the total energy consumption. For small uphill sections it is appreciated a similar behaviour as the PnG technic, where the motor increases a little bit the electrical motor power before the top and then, it reduces the power to zero (coasting). Coasting is used for small negative slopes on the road, where the vehicle accelerates with zero power till the upper-speed limit is reached. However, for long negative slopes, the motor must use regenerative braking to not exceed the maximum speed. This concept is represented in more detail in Figure 13.

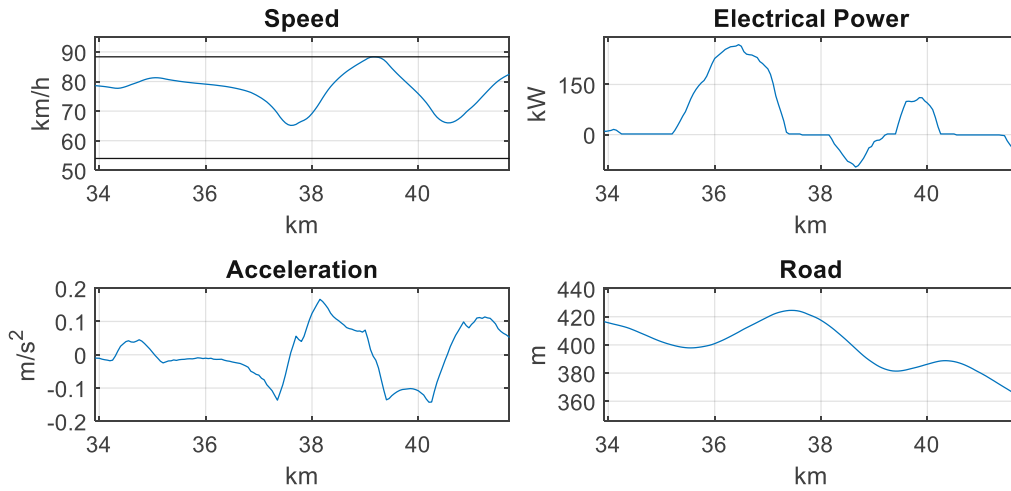


Figure 13: Behaviour similar than PnG for different slopes on the road from the optimal speed planning. Before the uphill the motor increases the electrical power and when the truck is almost at the top it starts the coasting.

These results are aligned with other different reports regarding eco-driving and optimal speed planning control [43,54]. The use of coasting sections instead of regenerative braking improves and reduces the total energy consumption of the vehicle. From the point of view of electrical power and efficiency, energy use is defined as the rate between the negative and the positive power as it is shown in the following equation.

$$\left| \frac{P_{e_{negative}}}{P_{e_{positive}}} \right| = \frac{Fw_{negative} \cdot v \cdot \eta}{\frac{Fw_{positive} \cdot v}{\eta}} = \eta^2 \quad (64)$$

This means that if the truck uses negative power, (regenerative power) instead of positive, the energy use increases by a factor of $1/\eta^2$. To prove this in the fuel truck of the thesis, and to observe the influence in energy consumption of this factor, it is performed a simulation with an ideal efficiency $\eta = 1$ to obtain the optimal speed planning without the effects of the energy use. As it was expected for this simulation, coasting sections are replaced by negative power sections and the speed remains

almost constant along the route. To analyse in terms of energy consumption this effect, it is calculated the energy consumption of this speed profile in the real model, and it is compared to the energy consumption from the optimal speed planning using the real efficiency. Results from this comparisons show an increase of 2.5% of the total energy without considering the efficiency of the motor in the optimal speed planning.

The smooth term is included in the objective function to improve driver comfort penalizing high-speed oscillations and promoting sections with steady speed.

$$\min \int_0^{s_f} (F_e + \lambda_t \frac{1}{v} + \lambda_{smooth} \vartheta + \psi) ds \quad (65)$$

This smooth term is represented as the difference between two consecutive speed intervals on the road $\vartheta = (v_k - v_{k-1})$ by a factor or smooth weight, λ_{smooth} . This factor is determined by the balance of a good speed profile without an increase in the motor energy consumption. By applying the smooth term in the objective function, sudden changes in speed and power profile are avoided, and oscillations in speed, acceleration, and electric motor power are reduced leading to a better driver comfort. Results from Figure 14 show the comparison of implementing or not the smooth term.

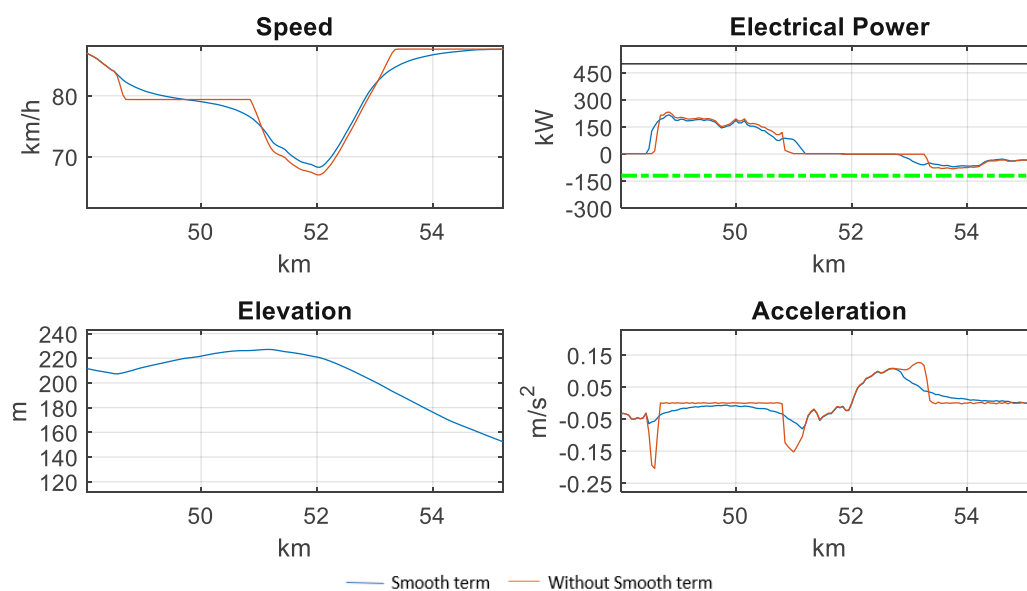


Figure 14: Comparative of the use of the smooth term in both strategies.

4.2. Evaluation of speed planning strategies

In this section, the differences between the strategies used to solve the optimal speed planning control are discussed in detail. Both strategies, using directly dynamic programming or implementing the synthesis of Pontryagin's minimum principle beforehand, present advantages and drawbacks. The parameters to evaluate the use of one or another strategy are energy consumption, computational time, and power, speed, and acceleration profiles.

4.2.1. Comparison of the speed and power profile over the total route for both strategies

To compare the use of the synthesis of Pontryagin's minimum principle prior to dynamic programming with using only dynamic programming, the route is simulated with the same trip time for both strategies, Figure 15 and Figure 16.

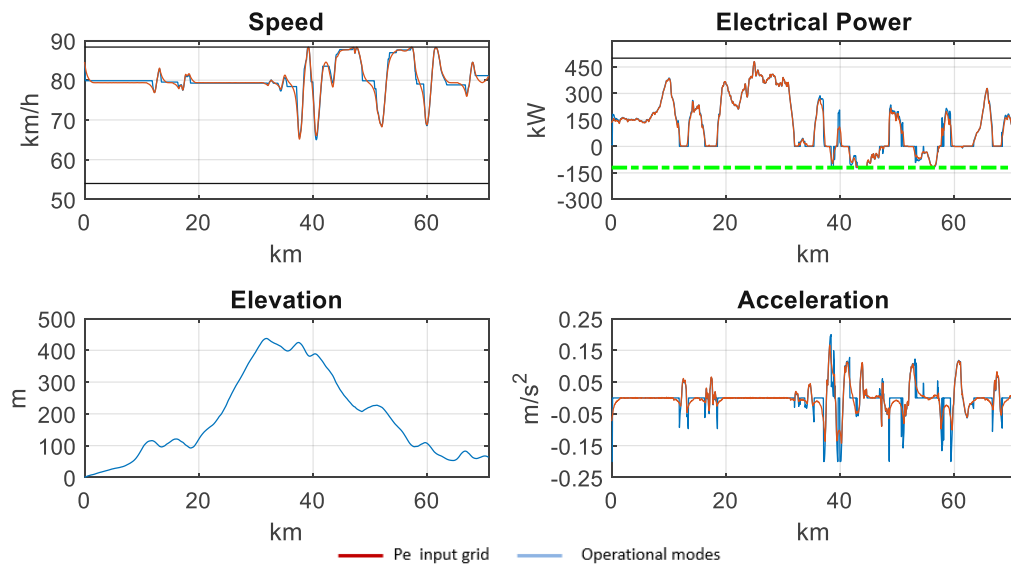


Figure 15: Results profiles comparative between both strategies

From these results, it is proven that both strategies follow the same trend. Speed and power profiles present similar results, but the main difference is the smoothness and spikes of the profiles. Using a wide control grid in dynamic programming let the optimization to adjust and obtain smoother profiles, meanwhile for the synthesis of Pontryagin's minimum principle an accurate control of the speed is not possible. Synthesis of Pontryagin's minimum principle leads the optimization to more steady speed sections, but also to more sharp speed changes and spikes in acceleration. This strategy would be useful to get an idea or a reference of the optimal power and speed profiles and an approximation of the total energy consumption for a specific trip time, however, it is not accurate enough if the driver must strictly adhere to it. The idea of

the speed profile is to be followed by a driver, so based on the results and plots in a real scenario it would be better to use directly dynamic programming with a wide control and state grid to obtain a balance between energy consumption, computational time, and speed and power smooth profiles.

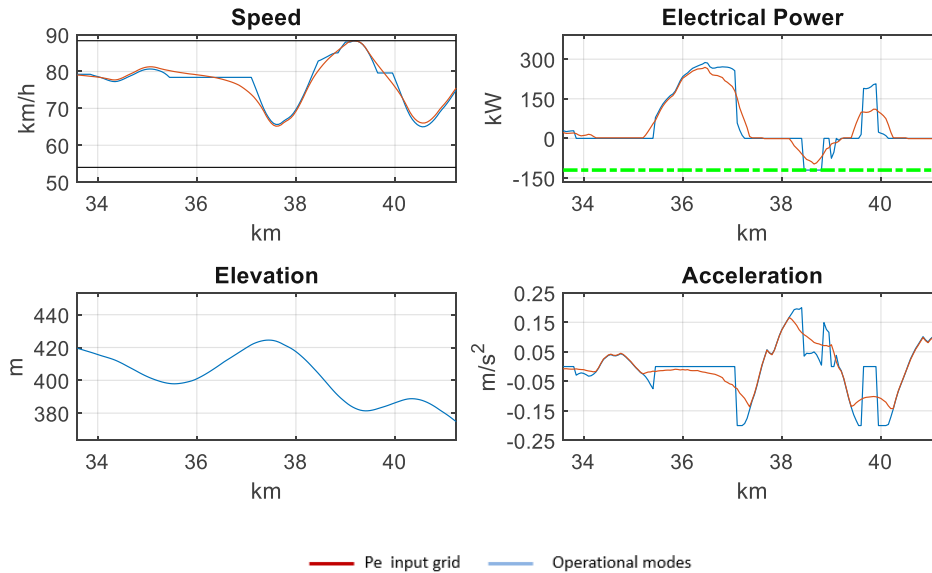


Figure 16: Zoom of a section in both strategies

4.2.2. Evaluation of energy consumption and computational time for both strategies

The main benefit of using the synthesis of Pontryagin's minimum principle is the reduction of the computational time. This is a factor to consider in some applications, where getting results quickly on the road is more important than the smoothness of the speed or power profile. Figure 17 shows the computational times and the energy consumption for both optimizations.

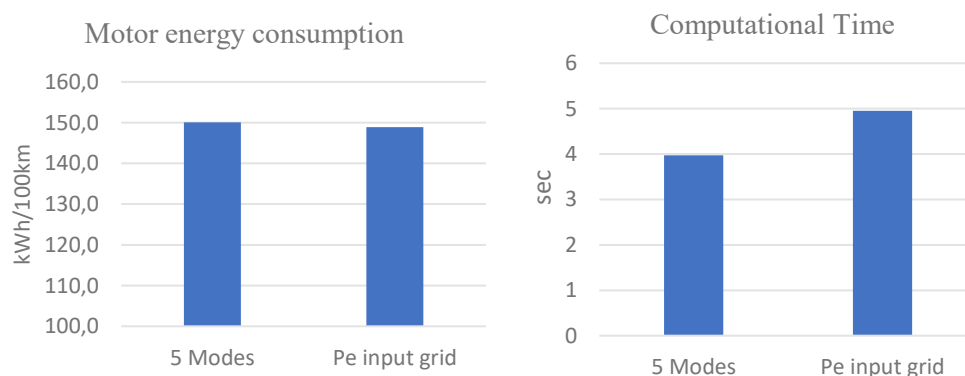


Figure 17: Comparison of motor energy consumption and computational time for both strategies

From these charts, it is confirmed that the synthesis of Pontryagin's minimum principle reducing the grid to 5 operational modes leads to faster computational times than using directly dynamic programming. However, the differences in computational time of both strategies are not very large, and both are fast enough to solve the optimal speed planning control if the grid is well designed. Energy consumption for both strategies is very similar as well, but with better results using directly dynamic programming because of the larger grid size.

Hence, it is concluded that for the following energy management simulations and the global optimization will be only used a wide control grid with P_e as the control variable. The synthesis of Pontryagin's minimum principle is discarded because both energy consumption and speed and power profiles get worse and the computational time without using it is fast enough for this application.

4.3. Optimal speed planning and energy management results

4.3.1. Analysis of results using power constraints

Once it is defined the optimization and the strategy to solve the optimal speed planning, the energy management control is implemented. The energy management control splits the electric motor power obtained from the optimal speed planning into fuel cell and battery power. The state of charge, SoC, is used as the state variable in the model and the fuel cell power as the control variable. Notice that all the simulations proposed in this work use the same initial and final SoC, therefore, the total battery energy remains around zero. From this control is obtained the fuel cell power, battery power, and the SoC profile, as well as the hydrogen consumption, which is the parameter to minimize in the objective function.

As it was observed in the optimal speed planning, the fuel cell electric truck uses high electrical motor power values along the uphill. Peaks in electric motor power, as well as the use of high values of power, lead to an increase in battery ohmic losses, equation (15). An increase in ohmic losses brings higher temperatures to the battery, therefore, the battery lifetime is reduced. To avoid this and improve the battery behaviour without an increase in the hydrogen and energy consumption, is implemented a soft constraint at 250 kW. This section explains the benefits of using soft power constraints in the optimal speed planning by evaluating the impact on ohmic losses from the energy management control. Simulations implementing soft power constraints and without constraints for the same trip time are shown in Figure 21.

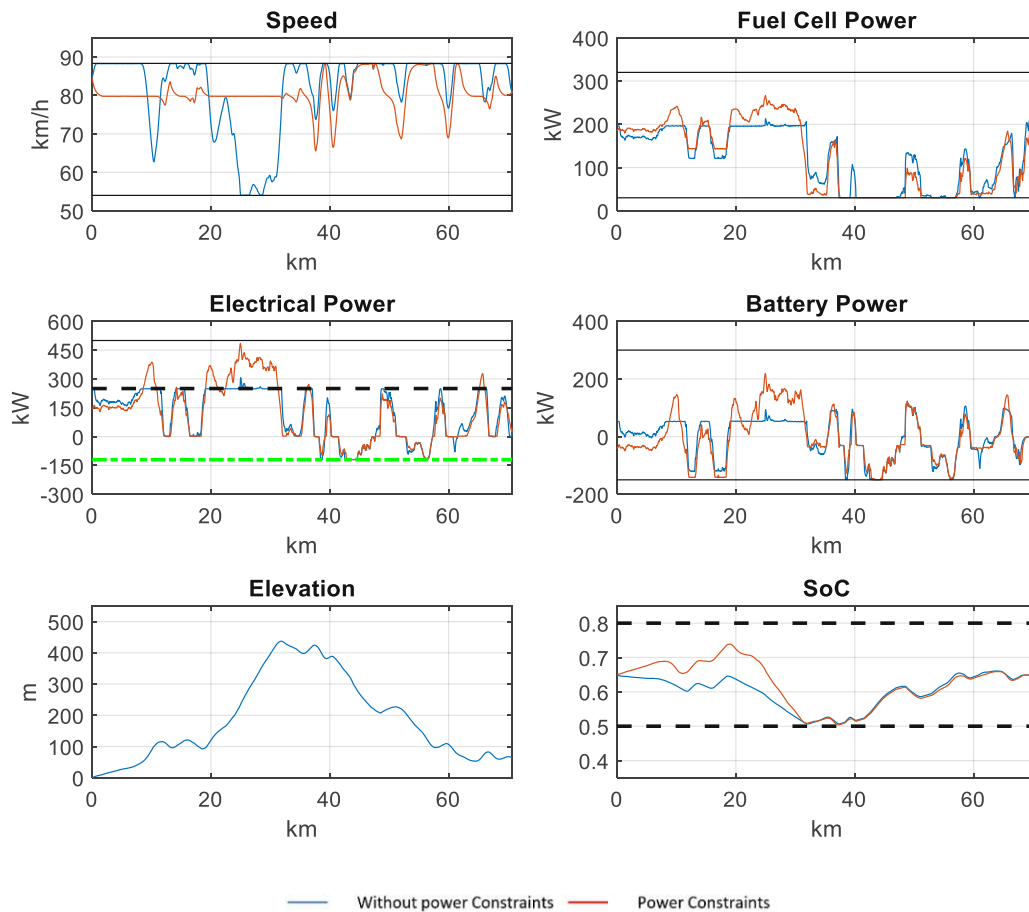


Figure 18: Optimal speed planning and energy management control results with and without soft power constraints at 250 kW.

Looking at the speed profile it can be observed that the speed distribution in the first part of the route is more constant without implementing soft power constraints to minimize energy consumption than using power constraints. The optimal speed profile implementing these power constraints uses the whole speed range within the speed limits. By penalizing high electrical motor power values, the power is reduced along the uphill and the motor only exceeds 250 kW when strictly necessary. This reduces the value of the ohmic losses and increases the battery lifetime. The optimization makes a balance between the cost associated with the penalties of high power and energy consumption and this causes that the speed profile is not constant anymore. The upper-speed limit is reached in several sections of the route, and the lower-speed limit is used along sections with high slope elevation values (from 20 km to 30 km). For negative slopes in downhills, high electric motor power is not required, so the speed profile for both simulations is similar. Regarding SoC from the simulations, the values without power constraints are higher than the values using this soft power constraint, but both are within the degradation limits of the battery. In order to give a better understanding of the relevance of the soft power constraints in our model and the behaviour of the system, it is presented the trade-off of the hydrogen consumption and ohmic losses over time, Figure 22 and Figure 23.

Simulations using penalties in electrical motor power present similar results in energy and hydrogen consumption but a high decrease in ohmic losses. For fast trips (less than 50 minutes) the differences in ohmic losses decrease over time because the weighting time factor in the objective function becomes much more relevant than the rest of the terms, so they are almost neglected to achieve these trip times. For standard trip times, (from 50 to 60 minutes), the differences in the ohmic losses are more significant. For these times, the soft power constraint is high enough in comparison with other terms in the objective function to influence the speed and power profiles. Optimizations by using soft power constraints at $0.5P_{e,max}$ and $0.75P_{e,max}$ could lead to a decrease in ohmic losses of around 30% and 10% respectively. Slow trips (more than 60 mins) present similar ohmic losses with and without these constraints as well as fast trips. When the trip time is very low, the optimization itself does not use high powers, since, for a slow driving, the high slope of the road is overcome without exceeding 250 kW. Minimizing energy consumption for a weighting time factor equal to or near to 0 results in similar speed and power profiles even if we use soft power constraints.

After the evaluation of the benefits of implementing the soft power constraints in the optimal control problem, this will be the base for the following simulations.

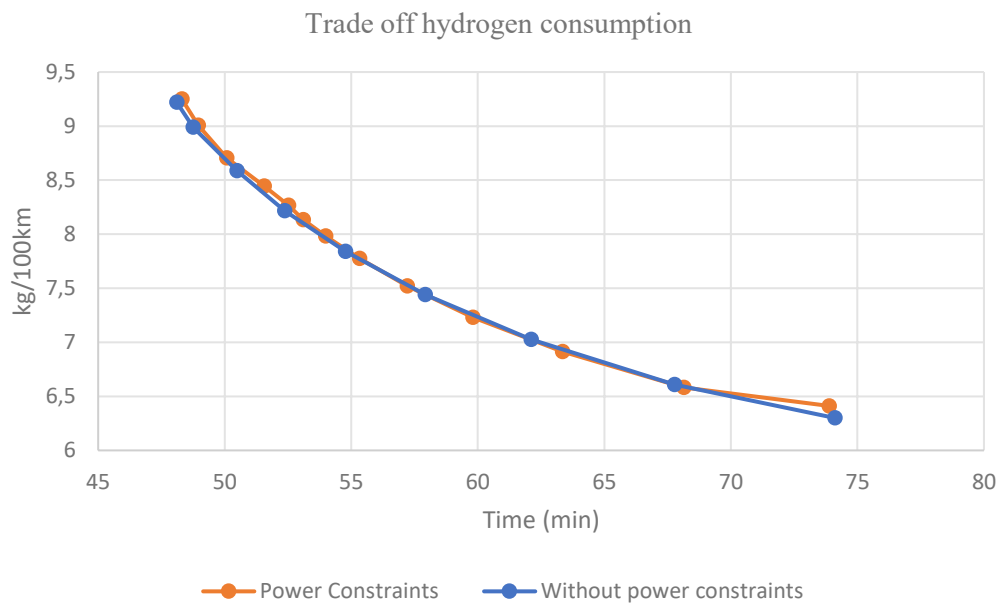


Figure 19: Comparison of hydrogen consumption using soft power constraints and without power constraints

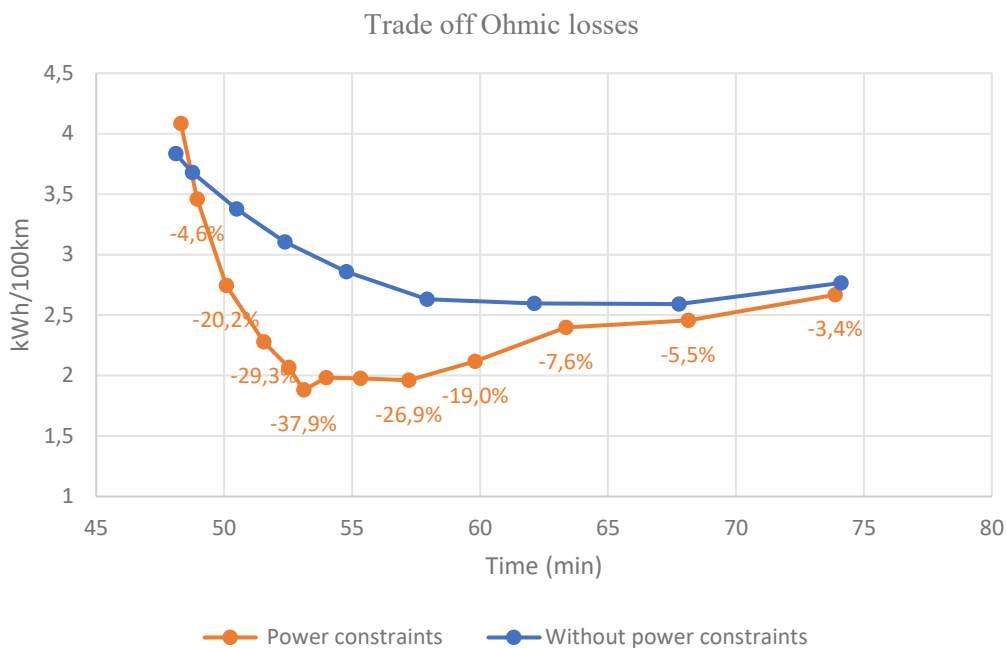


Figure 20: Comparison of ohmic losses using soft power constraints and without power constraints

4.3.2. Analysis of the effects of driving time over consumption

The main purpose of this master's thesis is to obtain a trade-off consumption over trip time. As we reduce the value of the weighted penalty on the trip time of the objective function, the average speed decreases in order to consume less electrical energy. Figure 18 shows the results from the optimal speed planning and energy management control for three different trip times. One difference between these three simulations is the range of speed used to minimize the total energy. For standard or long trip times, the speed range is wider and varies clearly along the route depending on the elevation and the slope of the road. On the other hand, for short trip times, the speed profile experiences fewer changes and remains around the upper limit value almost the whole route, since to achieve such trip time it is not possible to drive at low speed in any section of the road.

Regarding power profiles, the absolute value of electrical motor power for long trip times is always below the power for fast driving, and the soft power constraints are not exceeded. In addition, slow and standard driving present more sections using coasting than fast driving, and mechanical braking is not used. However, for fast trips, the minimum value of the regenerative power (-120 kW) is exceeded in some sections, increasing the total energy consumption, and high electric motor power values are used to keep up the speed along the uphill.

Similar behaviour is observed in the fuel cell power profiles, and battery power profiles. The range of battery power values used is wider for fast trips than for slow and standard trips, therefore the ohmic losses. Along the downhill, the fuel cell power for all simulations reaches the idle fuel cell power of 30 kW, and the battery provides or absorbs the power differences with respect to the electric motor. The main

differences are in the section of the high slope where the linear power limit is exceeded. Figure 19, Figure 20, and Table 5 analyse the energy and hydrogen consumption from the simulations for different trip times.

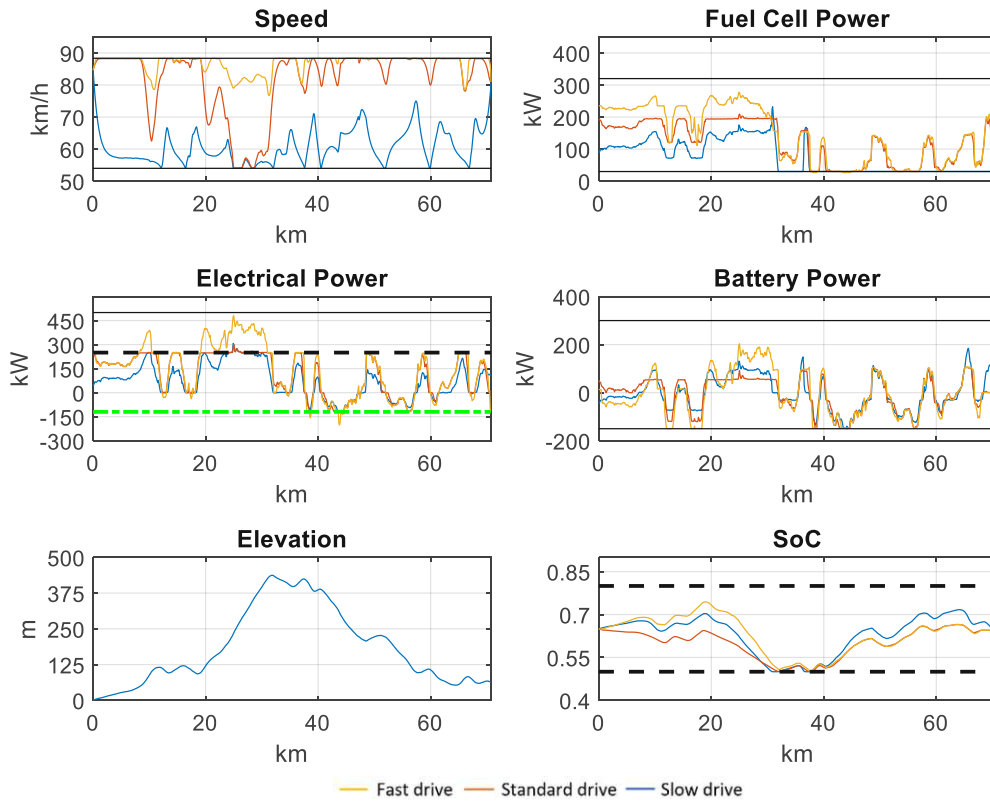


Figure 21: Energy management results for different trip times

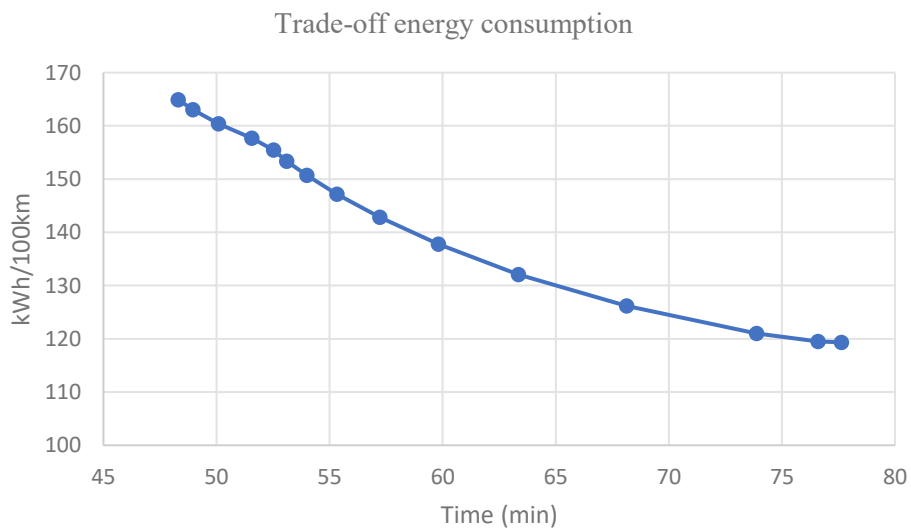


Figure 22: Trade-off energy consumption over time

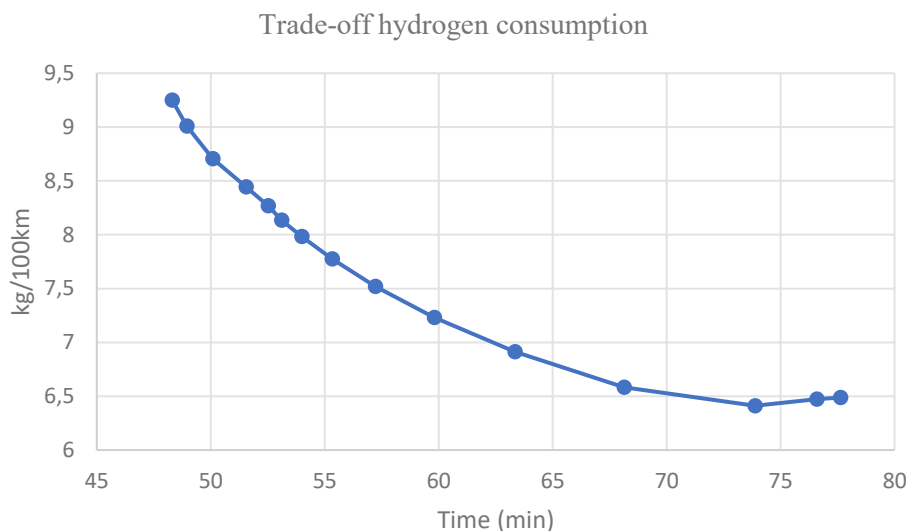


Figure 23: Trade-off hydrogen consumption over time

Effects in consumption increasing trip time			
	50 min	60 min	70 min
Energy (kWh/100km)	160,4	137,8 (-14%)	124,5 (-22%)
Hydrogen (kg/100km)	9	7,3 (-19%)	6,2 (-28%)

Table 5: Decrease of consumption for 60 min and 70 min trip time respect to 50 min

4.3.3. Evaluation of results for different elevation profiles

The total energy consumption of the fuel cell truck as well as the ohmic losses, and hydrogen consumption depend on the elevation profile of the route. Consumption on routes with high slopes (uphill and downhill) increases with respect to flatter ones. In this section, energy consumption, hydrogen consumption, and ohmic losses are analysed for two different driving cycles. The first driving cycle consists of an uphill with high slopes on the elevation. This driving cycle is the same as the one used for the rest of the simulations of the thesis, but the start and end points of the route are modified to match their values as it is explained in chapter 2. The second driving cycle is a flatter real cycle with small slopes in the elevation. As in the first driving cycle, the start and end elevation of the route match their values. To evaluate these two cycles, firstly the trade-off energy consumption over trip time is calculated by the optimal speed planning for each driving cycle, and energy management control is performed afterward.

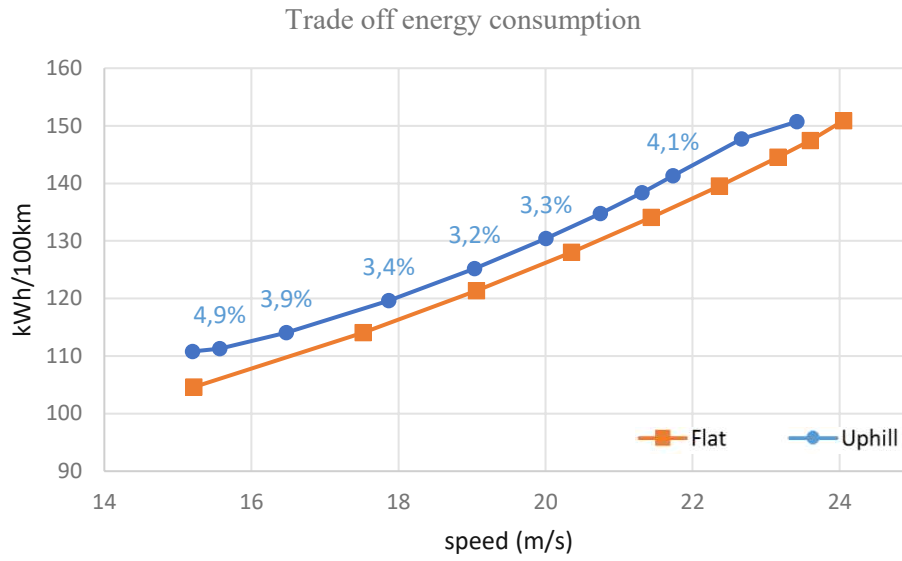


Figure 24: Electric motor energy consumption on an uphill and a flat route.

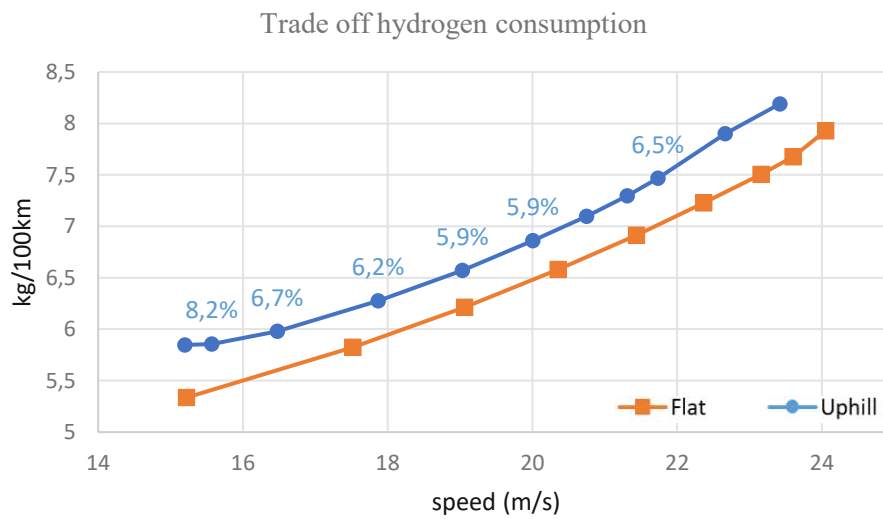


Figure 25: Hydrogen consumption on an uphill and flat route.



Figure 26: Ohmic losses on an uphill and flat route

Increase of consumption in uphill respect flat drive cycles (%)		
Motor Energy	Hydrogen	Ohmic losses
3.3 – 4.9	5.9 – 8.2	35 – 172

Table 6: : Increase of consumption from an uphill respect to flat route

The trade-off is represented in Figure 24, Figure 25, and Figure 26 and the main values for each parameter are indicated in Table 6. Results from the energy management control show an increase of 3.3-4.9 % in energy consumption, 5.5-8 % in hydrogen consumption, and an increase of 35-172 % in ohmic losses with respect to the flat cycle.

4.3.4. Analysis of results for different vehicle loads

Vehicle load is one of the most influential factors in the energy and hydrogen consumption of the fuel cell truck. Speed and power profiles for a specific time using different loads differ greatly, affecting energy and hydrogen consumption. Results in Figure 31 show that the speed profile using lighter loads presents a similar behaviour as without using power constraints. Speed remains constant during the high slopes of elevations and oscillates on negative slope sections. The lower speed limit is reached by the truck for full load during the high slope on the road, but for partial load, the speed does not go below 70 km/h. On the other hand, the upper-speed limit is reached in both simulations.

The main difference in the electrical power is regarding the power constraints. The truck with a full load of 40 tonnes, exceeds 250 kW to overcome the high slopes of the road, meanwhile, the truck with a partial load of 20 tonnes, is able to drive the whole route without exceeding that limit. This leads to a decrease in battery power and ohmic losses, as it is observed in Figure 28. Another observation from the results regarding electric motor power is that not only high positive electric powers are reduced, but also the use of regenerative power or the absolute value of negative powers which in turn is beneficial for ohmic losses. The fuel cell power used for a partial load is almost half of the power used by a truck with a full load along the uphill. Along the negative slope (downhill) is almost zero for both loads as in other simulations. The battery power is analysed in terms of the range of the power (maximum and minimum battery power values) since high absolute battery power values lead to higher values of ohmic losses. The heavy-duty vehicle with a full load uses a wider range of battery power values, as was expected, increasing ohmic losses which will cause more heating in the batteries reducing their lifetime. Finally, SoC behaviour is similar for both vehicle loads. Simulations with a full load present higher values along the downhill because of the differences in the electrical power, but in any case, it exceeds the upper or lower degradation limit. The following figures show the trade-off energy, hydrogen consumption, and ohmic losses over the trip time for different vehicle loads.

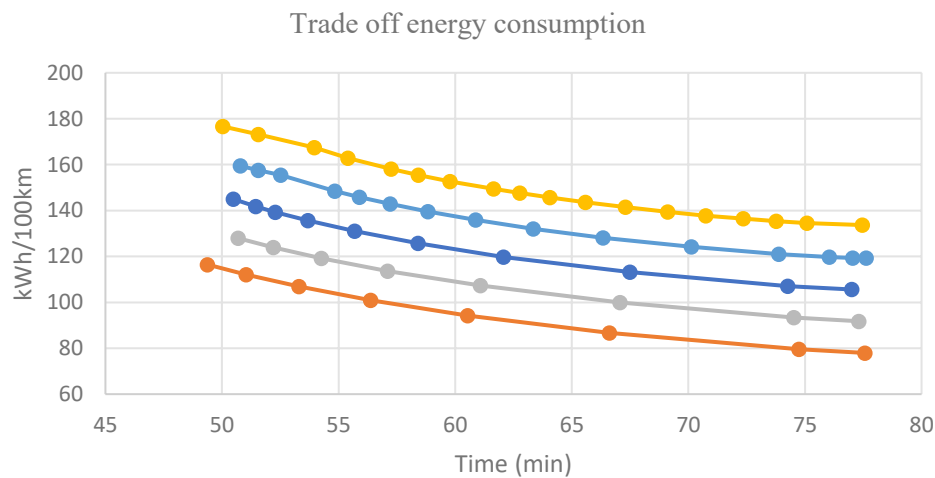


Figure 27: Electric motor energy for different vehicle loads

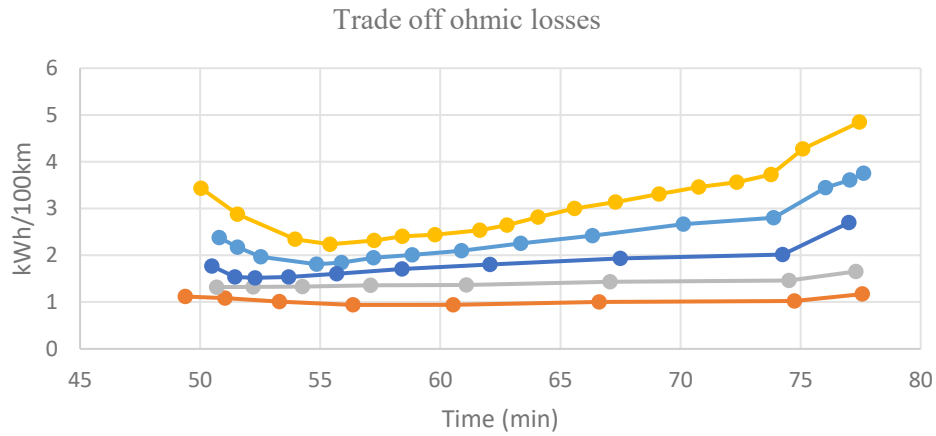


Figure 28: Ohmic losses for different vehicle loads

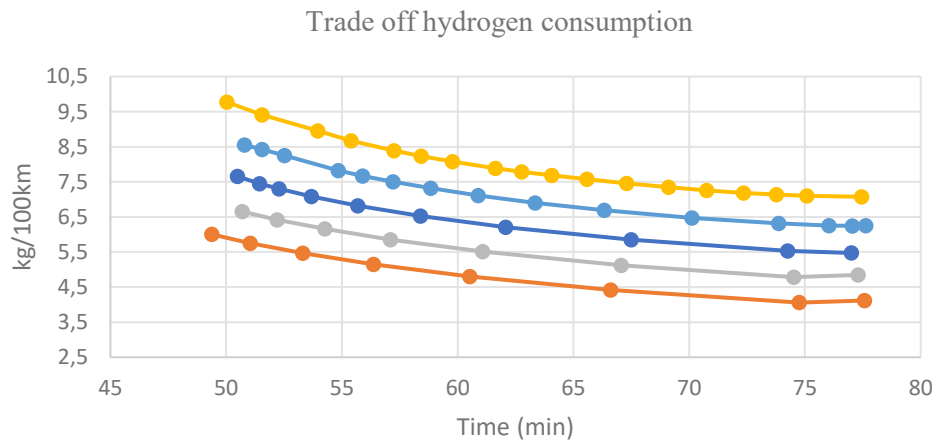


Figure 29: Hydrogen consumption for different vehicle loads

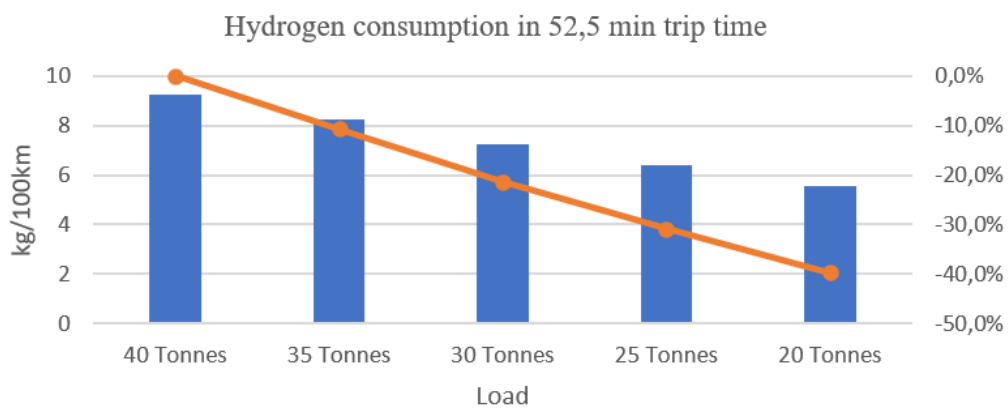


Figure 30: Comparison of hydrogen consumption respect to a full load 40 tonnes for a trip time of 52,5 min

From Figure 29 is calculated the decrease in hydrogen consumption respect to the full vehicle load as the truck load is reduced for the same trip time (52.5 minutes). It presents a linear behaviour with a reduction of 10% or 1kg/100km every 5 tonnes. The use of partial loads presents obvious benefits in both ohmic losses and hydrogen consumption for same trip times. Vehicle load is a major factor to consider by the customers for the feasibility of long trips by heavy-duty vehicles in order to optimize energy and hydrogen consumption as well as ohmic losses in the battery.

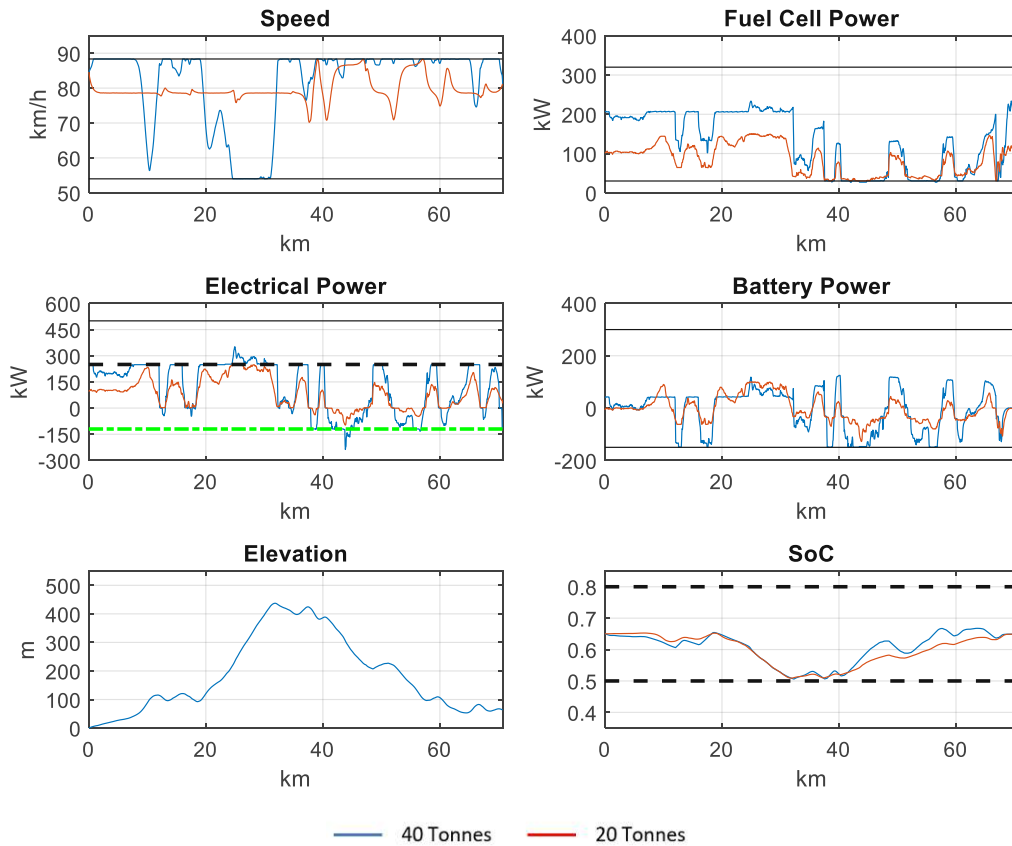


Figure 31: Comparison of profiles for full and partial vehicle loads.

4.3.5. Evaluation of results using different objective functions in the optimal speed planning and energy management

So far, optimal speed planning and energy management control allowed us to dive deep into energy and hydrogen consumption and battery behaviour for different scenarios (vehicle loads, elevation profiles, or penalizing high electric motor power values). For these simulations, it was always used the same terms in the objective functions of both optimal controls. In this chapter, it will be evaluated results from different objective functions in the optimal speed planning and energy management control to improve the battery behaviour without a significant increase in the hydrogen consumption.

This study is done by modifying one of the objective functions (optimal speed planning or energy management control) and keeping the other without any change with respect to the standard used in previous simulations. Then, the results are compared to the use of the standard objective functions in both optimizations.

4.3.5.1. Objective functions in the speed planning

For the purpose of obtaining a speed profile that improves the behaviour of the batteries reducing the ohmic losses, it was modelled an ideal battery with similar parameters as the real battery of the fuel cell electric truck in the optimal speed planning control. The battery consists of a constant ohmic resistance and an open circuit voltage ($R_{int} = 0.05\Omega$, $V_{oc} = 380V$). For the optimal speed planning, the battery system is considered the only source of power, so the battery power is equal to the electrical motor power. In this model, the internal resistance and open circuit voltage are independent of the SoC unlike in the optimal energy management control.

Two objective functions for the optimal speed planning are proposed to reduce the value of the ohmic losses without a high increase in energy and hydrogen consumption. The first objective function minimizes the ohmic losses by replacing the energy term with the ohmic losses, equation (66). As the ohmic losses are proportional to the square of the battery current, this term will penalize the absolute power value and not only high positive powers.

$$\min \int_0^{s_f} \left(\frac{P_{\Omega}}{v} + \lambda_t \frac{1}{v} + \lambda_{smooth} \vartheta + \psi \right) ds \quad (66)$$

The second objective function also reduces ohmic losses, but this time, the energy consumption term is replaced by the variation of the state of charge, equation (67). ΔSoC is proportional to the current, so using this term, only high positive values of electric load are considered to be minimized. This allows the optimization to obtain better results in terms of energy and hydrogen consumption but with lower ohmic losses drop than in the previous optimal control.

$$\min \int_0^{s_f} \left(\frac{-\Delta SoC}{v} + \lambda_t \frac{1}{v} + \lambda_{smooth} \vartheta + \psi \right) ds \quad (67)$$

Results from these new optimal speed planning controls are also introduced into the energy management control to calculate hydrogen consumption and final ohmic losses. The next figures show a comparison between results from the new objective functions and the reference objective function formulated in previous chapters.

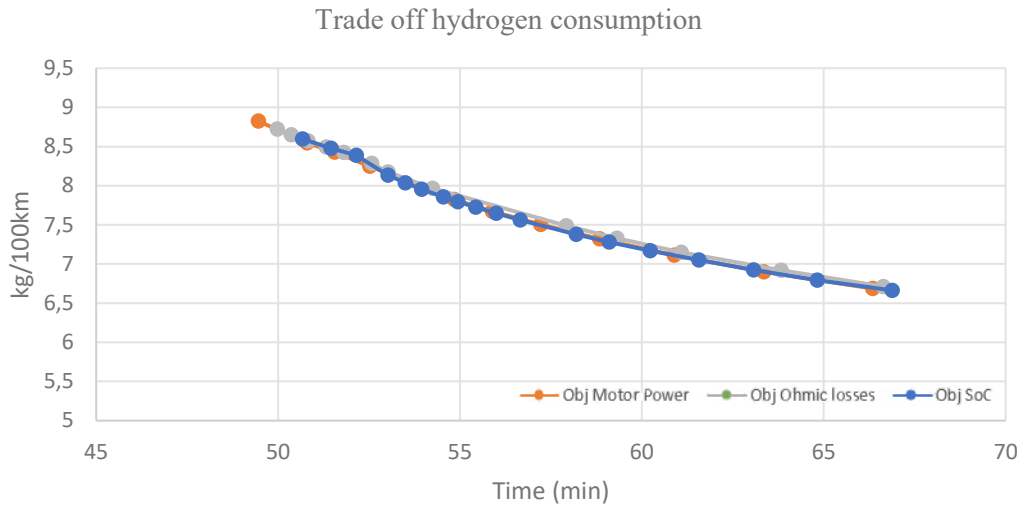


Figure 32: Hydrogen consumption results for different objectives functions in the speed planning

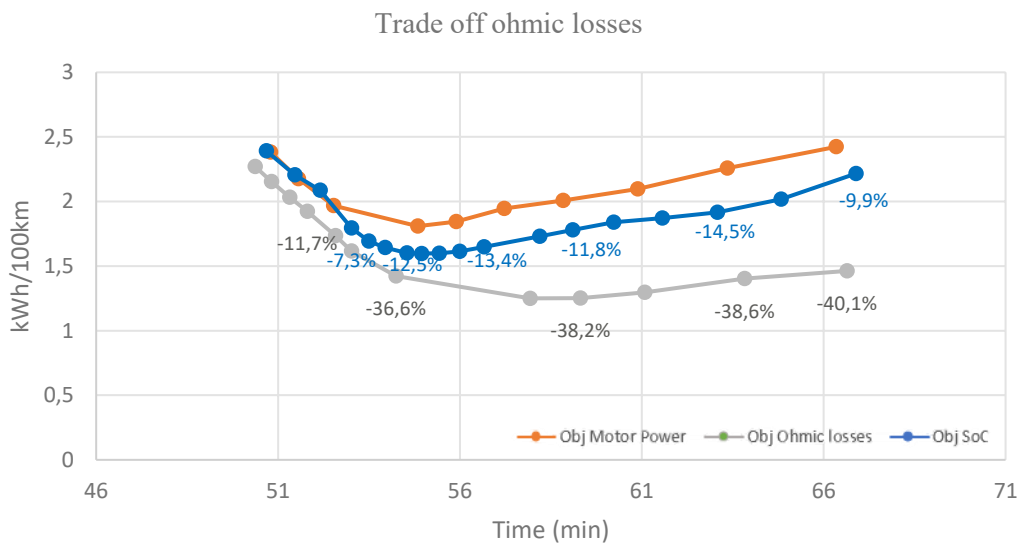


Figure 33: Ohmic losses for different objectives functions in the speed planning

Term in the objective function	Motor Energy %	Hydrogen %	Ohmic Losses %
ΔSoC	0.15	0	-12
P_{Ω}	1.5	0.1	-35

Table 7: Summary of results for two new objectives functions in the optimal speed planning after implementing an ideal battery in comparison to the standard objective functions from previous sections

By using ΔSoC and P_{Ω} in the objective function instead of the electrical motor power is achieved an improvement in the ohmic losses without a significant increment in the total motor energy or hydrogen consumption. These terms reduce around 12% and 35% ohmic losses respectively, while managing to maintain similar hydrogen consumption results than for previous simulations. As it was mentioned in other sections, for simulations with short trip times, results from different scenarios or terms in the objective function are more similar. This is caused by the high value of the weighting time factor, which makes the optimization focus only on the trip time, and the rest of the terms are almost neglected.

4.3.5.2. Objective functions in the energy management.

Simulations implementing a battery in the optimal speed planning and modifying the objective function proved that it is possible to obtain good hydrogen consumption and improve the battery behaviour of the fuel cell electric truck. In the following simulations, it will be used the standard optimal speed planning control, minimizing the total energy consumption, but the objective function of the energy management control is modified. The goal is the same as in the previous section, reduce ohmic losses without increasing the energy and hydrogen consumption. As the energy management control is the last step in the hierarchical optimization and it is implemented a real battery and fuel cell system, it could be expected to reduce even more the ohmic losses in comparison to the previous section but with an increase in the hydrogen consumption.

To achieve this, it is proposed to include the ohmic losses term in the objective functions as is represented by equation (68).

$$\min \int_0^{s_f} \frac{P_{\Omega}}{v} ds \quad (68)$$

Figure 34 represents the hydrogen consumption over time and in Figure 35 the ohmic losses. Finally, a summary of the results of different strategies in energy management is shown in Table 8.

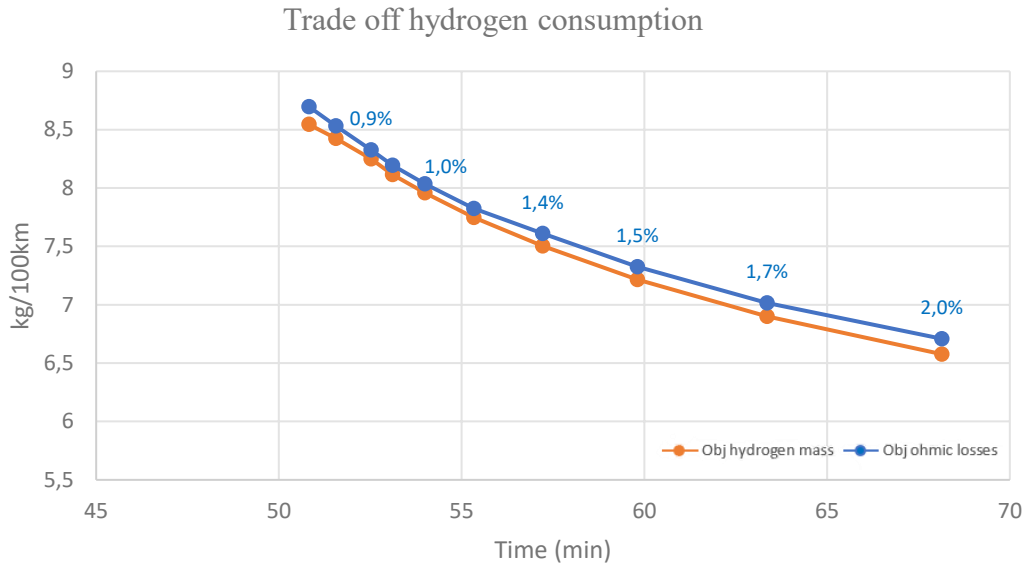


Figure 34: Hydrogen consumption results for different objectives functions in the energy management.

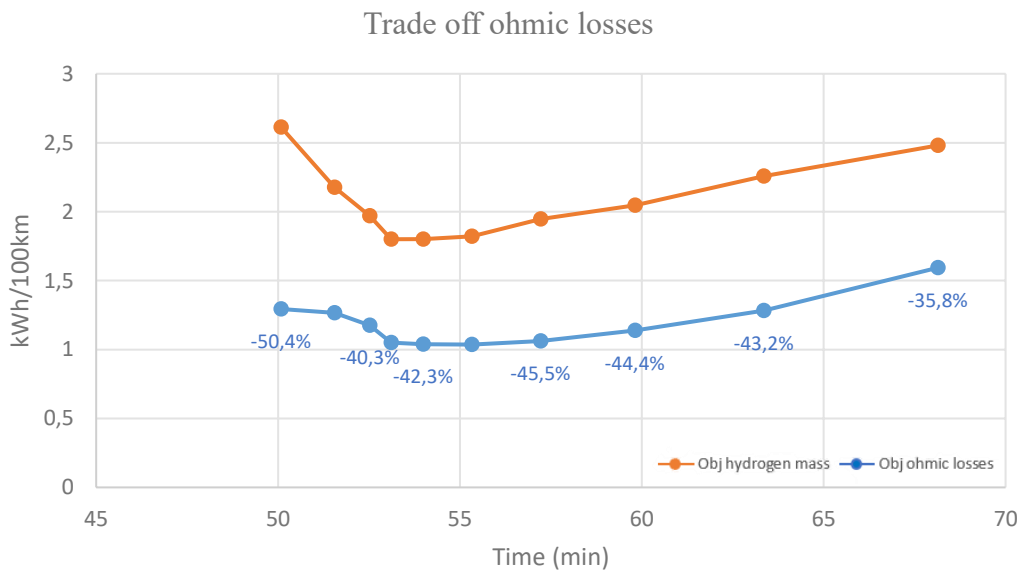


Figure 35: Ohmic losses results for different objectives functions in the energy management.

Term in the Objective function	Hydrogen %	Ohmic Losses %
P_{Ω}	1.5	- 45

Table 8: Summary of results for two new objectives functions in the energy management

The results confirm that it is possible to reduce further ohmic losses by modifying the objective function of the energy management control, but on the other hand, the impact in hydrogen consumption is higher. These results open a wide range of possible options for implementing and modelling the hierarchical optimization. Depending on the needs of the vehicle and the route, it should be done a proper study about the balance between the battery behaviour and the energy or hydrogen consumption before the trip to decide which objective function is most suitable according to the requirements. Finally, it is included a summary of all the results from both optimizations for a better understanding and overview of the effects of the different objective functions in Table 9.

Optimization	Objective function	Hydrogen %	Ohmic Losses %
Speed Planning	$-\Delta SoC$	0	(-5) - (-7)
	P_{Ω}	0.1	(-5) - (-9)
Energy Management	P_{Ω}	1.5-1.9	(-45) - (-52)

Table 9: Summary of results for new objectives functions in both speed planning and energy management

5. Conclusions

This thesis proposed the implementation of an optimal speed planning and energy management control for eco-driving of a fuel cell electric truck using dynamic programming. The strategy to solve the control problem is a hierarchical optimization, which breaks the global optimization into two sub-problems. and allows to minimize and analyse the energy and hydrogen consumption over driving time as well as to study the degradation of the battery based on the ohmic losses.

The trade-off energy and hydrogen consumption over trip time shows a significant decrease in energy and hydrogen consumption by increasing the trip time. For standard or long trip times, the speed range is wider than for fast trips and varies clearly along the route depending on the elevation and the slope of the road. The electrical motor power profiles also differ depending on the trip time. Faster trip times require more power, and the soft power constraints at 250 kW must be exceeded in order to achieve high speeds along the uphill. This also affects negative electrical power values, since for fast trips is used mechanical braking instead of only coasting and regenerative braking.

Results show that mechanical braking could be completely avoided to reduce energy and hydrogen consumption if the driving time is not too short. It is replaced by regenerative braking and coasting to slow down the fuel cell electric truck. By regenerative braking the energy from the wheels to the motor can be re-used in the system, however, simulations indicate that for small uphill sections it is better to use the PnG technic, where the motor increases the power before the top and then reduce the power to zero (coasting) to decrease the speed. It could happen that the hill had a long negative slope very steep, so the electric motor must employ the use of regenerative braking to avoid exceed speed limits.

Another important study is the influence of the vehicle load in the hydrogen consumption for same driving times. It is observed a linear behaviour with a reduction of 10% or 1kg/100km every 5 tonnes reduction in the truck load. The use of partial loads benefits battery lifetime and hydrogen consumption.

This master's thesis approaches different methods to reduce ohmic losses. By including soft power constraint in the optimal speed planning control are achieved lower values of electrical power of the motor which lead to a reduction of ohmic losses. For standard trip times is obtained similar energy and hydrogen consumption results and a significant reduction of ohmic losses. Very fast or slow driving leads to similar results with or without these penalties. In fast trips, the weighting time factor is so high that the rest of the terms are almost neglected, including the soft power penalties, and for slow trips, the optimization itself does not use high power values in any section, so the results are the same.

In addition, the use of different objective functions in the optimal speed planning and energy management control regarding the study of the ohmic losses show considerable benefits. By modelling an ideal battery in the optimal speed planning

and including the ohmic losses or the variation of the state of charge in the objective function is decreased around 8% ohmic losses without an increment in hydrogen consumption. On the other hand, changes in the objective function of the energy management control could achieve reductions of up to 50% of ohmic losses increasing only around 1.5% hydrogen consumption. This opens new possibilities for driving behaviours to try to reduce only hydrogen consumption or a mix of both battery lifetime and hydrogen consumption.

From this master's thesis, it is also concluded that the synthesis of Pontryagin's minimum principle is a good approximation to obtain the speed distribution along the road to minimize the energy consumption of the fuel cell electric truck. Reducing the control grid to 5 leads to a decrease in computational time. However, it was proved that the use of this strategy for the case of this work is not necessary, because by choosing a proper control grid size using only dynamic programming is possible to achieve good enough computational times. In addition, the speed and power profiles from this strategy are less realistic with more ups and downs and spikes in the acceleration, meanwhile, for the second one is obtained better speed and power profiles to be followed by the driver.

The optimization in this master's thesis is an offline model but it could easily be adapted to online models using GPS data. Dynamic programming gives us a look-up table of the speed distribution from the backward loop to minimize the energy or hydrogen consumption, so if we had the current speed and the location of the vehicle on the road, it should only be recalculated the forward loop of the optimization from the new start point, which does not require a large computational effort. All of this, in combination with a more realistic and complex model of the fuel cell electric truck and the road would be good future trends to study providing more insight into this topic.

6. Bibliography

[1] *Perspective of Clean Mobility in Road Freight Transport. Horizons of Railway Transport 2020.* Assoc. Prof. Ing. Helena Bínová, Ph.D, Mgr. Oldřich Hykšb , RNDr. Magdalena Hykšová, Ph.D , Assoc. Prof. Ing. Kristýna Neubergová, Ph. D, Ing. František Kekulac, Ing. Jindřich Sadil, Ph.D, (2021).

[2] 6.4. *Suspended particulates (TSP/SPM).* European Environment Agency. Date accessed on July 2, 2022. <https://www.eea.europa.eu/publications/2-9167-057-X/page021.html>

[3] *European Commission, Directorate-General for Mobility and Transport, EU transport in figures : statistical pocketbook 2021, Publications Office, 2021, <https://data.europa.eu/doi/10.2832/27610>*

[4] *Annual European Union greenhouse gas inventory 1990-2020 and inventory report 2022.* European Environment Agency. (27 May 2022)

[5] IEA (2022), *Global Energy Review: CO2 Emissions in 2021*, IEA, Paris <https://www.iea.org/reports/global-energy-review-co2-emissions-in-2021-2>

[6] Junevičius, R., Jackiva, I., Gopalakrishnan, K., Prentkovskis, O., & Cecco, D. (2020). *Transbaltica Xi: Transportation Science and Technology.* Springer International Publishing. <https://doi.org/10.1007/978-3-030-38666-5>

[7] *A Review of Heavy-Duty Vehicle Powertrain Technologies: Diesel Engine Vehicles, Battery Electric Vehicles, and Hydrogen Fuel Cell Electric Vehicles.* Carlo Cunanan, Manh-Kien Tran , Youngwoo Lee, Shinghei Kwok, Vincent Leung and Michael Fowler.(1 June, 2021)

[8] *International Council on Clean Transportation. 2022. The ever-improving efficiency of the diesel engine - International Council on Clean Transportation.* [online] Available at: <<https://theicct.org/the-ever-improving-efficiency-of-the-diesel-engine/#:~:text=Modern%20compression%20Dignition%20diesel%20engines,on%202013%E2%80%932014%20certified%20engines>> [Accessed 13 May 2022]

[9] E. (2021, July 6). *EV Powertrain Components - Basics.* EVreporter. Accessed (June 2022). <https://evreporter.com/ev-powertrain-components/>

[10] *EV database. (s/f). EV Database.* <https://ev-database.org/cheatsheet/range-electric-car>

[11] *Does Size Matter? The Influence of Size, Load Factor, Range Autonomy, and Application Type on the Life Cycle Assessment of Current and Future Medium- and Heavy-Duty Vehicles* Romain Sacchi, * Christian Bauer, and Brian L. Cox

[12] *Nikola Motor Company. 2022. Nikola Tre: Battery-Electric Daycab Semi-Truck.* [online] Available at: <<https://nikolamotor.com/tre-bev>> [Accessed 5 June 2022].

- [13] *Electric, V., VNR, V., VNL, V., VNX, V., VHD, V., VAH, V., Efficiency, F., X15, C., Transmission, I., Gas, N., Magazine, V. and Releases, P., 2022. VNR Electric. [online] Volvotrucks.us. Available at: <<https://www.volvotrucks.us/trucks/vnr-electric/>> [Accessed 5 June 2022].*
- [14] Porter, E. (2022, mayo 16). *If most truck journeys are less than 300 miles the E-Truck revolution can happen now. Energy Post. <https://energypost.eu/if-most-truck-journeys-are-less-than-300-miles-the-e-truck-revolution-can-happen-now/>*
- [15] *Stories, N. and trucks, C., 2022. Why an electric truck needs a charging strategy. [online] Volvotrucks.com. Available at: <<https://www.volvotrucks.com/en-en/news-stories/insights/articles/2021/nov/How-a-good-charging-strategy-can-extend-an-electric-trucks-range.html>> [Accessed 4 May 2022].*
- [16] *Es.helienergy.com. 2022. Estación de carga rápida de 300 kW para coches y camiones eléctricos | Heliox. [online] Available at: <<https://es.helienergy.com/products/rapid-300-kw>> [Accessed 8 July 2022].*
- [17] Shen, X.; Liu, H.; Cheng, X.; Yan, C.; Huang, J. *Beyond lithium ion batteries: Higher energy density battery systems based on lithium metal anodes. Energy Storage Mater.* 2018, 12, 161–175.
- [18] *The Money © - N°1 Official Money & Networth Source. 2022. Is fuel cell energy the future? [online] Available at: <<https://themoney.co/is-fuel-cell-energy-the-future/>> [Accessed 10 May 2022].*
- [19] *Volvo Trucks showcases new zero-emissions truck. (s/f). Volvotrucks.com. <https://www.volvotrucks.com/en-en/news-stories/press-releases/2022/jun/volvotrucks-showcases-new-zero-emissions-truck.html>*
- [20] *Edwards, R.; Larivé, J.F.; Beziat, J.C. Well-To-Wheels Analysis of Future Automotive Fuels and Power Trains in the European Context; Publications Office: Luxembourg, 2011.*
- [21] *Huang, W.D.; Zhang, Y.H.P. Energy efficiency analysis: Biomass-to-wheel efficiency related with biofuels production, fuel distribution, and powertrain systems. PLoS ONE* 2011, 6, 1–10.
- [22] *Optimizing Areal Capacities through Understanding the Limitations of Lithium-Ion Electrodes. Kevin G. Gallagher^{4,5,1}, Stephen E. Trask¹, Christoph Bauer², Thomas Woehrle², Simon F.Lux^{4,3}, Matthias Tschech², Peter Lamp², Bryant J. Polzin¹, Seungbum Ha¹, Brandon Long. (10 November 2015).*
- [23] *Toheed Ghandriz, Bengt Jacobson, Leo Laine, Jonas Hellgren, Impact of automated driving systems on road freight transport and electrified propulsion of heavy vehicles, Transportation Research Part C: Emerging Technologies, Volume 115, 2020.*

- [24] Chatti, Walid. (2021). *Moving Towards Environmental Sustainability: Information and Communication Technology (ICT), Freight Transport, and CO2 Emissions*. *Heliyon*. 7. 1-8. 10.1016/j.heliyon.2021.e08190.
- [25] *Vehicle Trajectory Optimization for Application in Eco-Driving*. Felicitas Mensing, Rochdi Trigui, Eric Bideaux (21 October, 2021)
- [26] YIXING LIU, *A Parallel Computing Implementation of Dynamic Programming and Its Application to an HEV*. Degree project in mechanical engineering, second cycle KTH Royal Institute of technology industrial engineering and management.
- [27] Hadi Abbas Youngki Kim, Jason B. Siegel, Denise M. Rizzo. *Synthesis of Pontryagin's Maximum Principle Analysis for Speed Profile Optimization of All-Electric Vehicles*. (11 March 2019)
- [28] S. Xu, S. E. Li, K. Deng, S. Li and B. Cheng, "A Unified Pseudospectral Computational Framework for Optimal Control of Road Vehicles," in *IEEE/ASME Transactions on Mechatronics*, vol. 20, no. 4, pp. 1499-1510, Aug. 2015.
- [29] S. Xu, S. E. Li, B. Cheng and K. Li, "Instantaneous Feedback Control for a Fuel-Prioritized Vehicle Cruising System on Highways With a Varying Slope," in *IEEE Transactions on Intelligent Transportation Systems*, vol. 18, no. 5, pp. 1210-1220, May 2017.
- [30] Manne Held, Oscar Flärdh, Fredrik Roos, and Jonas Martensson. *Implementation of an Optimal Look-Ahead Controller in a Heavy-Duty Distribution Vehicle*. 2019 IEEE Intelligent Vehicles Symposium (IV) Paris, France. June 9-12, 2019.
- [31] A. Sciarretta, G. De Nunzio and L. L. Ojeda, "Optimal Ecodriving Control: Energy-Efficient Driving of Road Vehicles as an Optimal Control Problem," in *IEEE Control Systems Magazine*, vol. 35, no. 5, pp. 71-90, Oct. 2015
- [32] *Trajectory optimization for eco-driving taking into account traffic constraints*. *Transportation Research Part D*, Felicitas Mensing, Eric Bideaux, Rochdi Trigui, Helene Tattegrain. (2012)
- [33] *Look-ahead control for heavy trucks to minimize trip time and fuel consumption*. Erik Hellström, Maria Ivarsson, Jan Aslund, Lars Nielsen. (15 August 2008)
- [34] Froberg, Anders & Hellström, Erik & Nielsen, Lars. (2006). *Explicit Fuel Optimal Speed Profiles for Heavy Trucks on a Set of Topographic Road Profiles*. *SAE Technical Papers*.
- [35] *Optimal Powertrain Control of a Heavy-Duty Vehicle Under Varying Speed Requirements*. Anders Froberg, Erik Hellström, Lars Dencker Nielsen. (January, 2021)

- [36] Hong Tu Luu, Lydie Nouvelière, Said Mammar, (July, 2010), *Dynamic Programming for fuel consumption optimization on light vehicle. 6th IFAC Symposium Advances in Automotive Control.*
- [37] Guo, Q., Zhao, Z., Shen, P. et al. *Optimization management of hybrid energy source of fuel cell truck based on model predictive control using traffic light information. Control Theory Technol.* 17, 309–324 (2019).
- [38] Liangfei Xu, Jianqiu Li, Minggao Ouyang, Jianfeng Hua, Geng Yang, *Multi-mode control strategy for fuel cell electric vehicles regarding fuel economy and durability, International Journal of Hydrogen Energy, Volume 39, Issue 5, 2014, Pages 2374-2389,*
- [39] Saman Ahmadi, S.M.T. Bathaee, *Multi-objective genetic optimization of the fuel cell hybrid vehicle supervisory system: Fuzzy logic and operating mode control strategies, International Journal of Hydrogen Energy, Volume 40, Issue 36, 2015.*
- [40] Alessandro Ferrara, Stefan Jakubek, Christoph Hametner, *Energy management of heavy-duty fuel cell vehicles in real-world driving scenarios: Robust design of strategies to maximize the hydrogen economy and system lifetime, Energy Conversion and Management, Volume 232, 2021.*
- [41] Gunter Heppeler, Marcus Sonntag, Oliver Sawodny. *Fuel Efficiency Analysis for Simultaneous Optimization of the Velocity Trajectory and the Energy Management in Hybrid Electric Vehicles. Preprints of the 19th World Congress The International Federation of Automatic Control Cape Town, South Africa. August 24-29, 2014*
- [42] Guo Jinquan, He Hongwen, Li Jianwei, Liu Qingwu, *Real-time energy management of fuel cell hybrid electric buses: Fuel cell engines friendly intersection speed planning, Energy, Volume 226, 2021.*
- [43] Youngki Kim, Miriam Figueroa-Santos, Niket Prakash, Stanley Baek, Jason B. Siegel, Denise M. Rizzo, *Co-optimization of speed trajectory and power management for a fuel-cell/battery electric vehicle, Applied Energy, Volume 260, 2020.*
- [44] Djamaledine Maamria, Kristan Gillet, Guillaume Colin, Yann Chamaillard, Cédric Nouillant. *Computation of eco-driving cycles for Hybrid Electric Vehicles: Comparative analysis. Control Engineering Practice, Elsevier, 2018, 71, pp.44-52.*
- [45] JAMA (Japan Automobile Manufacturers Association, Inc.): *Reducing CO2 Emissions in the Global Road Transport Sector, PDF (2008).*
- [46] Hiraoka, Toshihiro & Terakado, Yasuhiro & Matsumoto, Shuichi & Yamabe, Shigeyuki. (2009). *Quantitative evaluation of eco-driving on fuel consumption based on driving simulator experiments.*
- [47] J. Lee, D. Nelson, H. Lohse-Busch, “*Vehicle Inertia Impact on Fuel Consumption of Conventional and Hybrid Electric Vehicles Using Acceleration and Coast Driving Strategy,*” in *Proc. of SAE World Cong. & Exhibition, Detroit, USA, 2009.*

[48] *Strategies to Minimize Fuel Consumption of Passenger Cars during Car-Following Scenarios*. Shengbo Eben Li and Huei Peng. 2011 American Control Conference on O'Farrell Street, San Francisco, CA, USA June 29 - July 01, 2011

[49] EVCARTIPS. (2020, enero 23). Do electric cars idle? EV Car Tips. <https://evcartips.com/do-electric-cars-idle-%EF%BB%BF/>

[50] Rolling resistance. Engineering ToolBox. (n.d.). Retrieved June 15, 2022, from https://www.engineeringtoolbox.com/rolling-friction-resistance-d_1303.html

[51] 1.2.2 lecture notes: Sizing of the EV power train. TU Delft OCW. (2020, February 28). Retrieved June 13, 2022, from <https://ocw.tudelft.nl/course-readings/1-2-2-lecture-notes-sizing-of-the-ev-power-train/>

[52] *Exact and Approximate Dynamic Programming Principles*. Available at: http://web.mit.edu/dimitrib/www/RL_1_NEW_BOOK.pdf Accessed 26 November 2021.

[53] Taylor, C. R. (2019). *Applications Of Dynamic Programming To Agricultural Decision Problems*. United States: CRC Press.

[54] M. Held, O. Flärth and J. Mårtensson, "Optimal Speed Control of a Heavy-Duty Vehicle in Urban Driving," in *IEEE Transactions on Intelligent Transportation Systems*, vol. 20, no. 4, pp. 1562-1573, April 2019

7. Appendix

Synthesis of Pontryagin's principle applied to the model

Objective function: Minimize total energy consumption

$$J = \int_0^{t_f} \frac{P_e}{m_v} dt = \int_0^{t_f} \left(\frac{xu_1}{\eta_1} + xu_2\eta_2 \right) dt$$

State variable:

$$x = v$$

$$\dot{x} = \frac{dv}{dt} = u_1 + u_2 + u_3 - f_{res}(x)$$

Control inputs:

$$u = [u_1, u_2, u_3] = \left[\frac{Fm}{m_v}, \frac{F_g}{m_v}, \frac{F_b}{m_v} \right]$$

Resistance force:

$$F_{roll} = m_v g c_r \cos \alpha$$

$$F_{slope} = m_v g \sin \alpha$$

$$F_{drag} = \frac{1}{2} A_v c_x \rho_{air} v^2$$

$$f_{res} = A + Bx^2$$

$$A = \frac{F_{roll} + F_{slope}}{m_v}, \quad B = \frac{A_v c_x \rho_{air}}{2m_v}$$

Ad-joint equations:

$$\dot{p} = -\frac{\partial H}{\partial x} = -\frac{u_1}{\eta} - u_2\eta + 2pBx$$

Factorize the input u to determine the driving operational modes:

$$H = \left(\frac{x}{\eta} + p\right)u_1 + (x\eta + p)u_2 + pu_3 - pf_{res}(x)$$

Then we have $3^3 = 27$ options because we have three input variables and three different cases for each one (less, equal or greater than zero). However, there are some infeasible cases due to the values of the efficiency of the moto $0 \leq \eta \leq 1$, the behaviour of the vehicle $x > 0$ and mathematical operations. Therefore, PMP lead only to 7 cases.

$$\frac{x}{\eta} + p < 0, x\eta + p < 0, p < 0 : u = [\overline{u_1}, 0, 0]$$

$$\frac{x}{\eta} + p > 0, x\eta + p < 0, p < 0 : u = [0, 0, 0]$$

$$\frac{x}{\eta} + p > 0, x\eta + p > 0, p < 0 : u = [0, \underline{u_2}, 0]$$

$$\frac{x}{\eta} + p > 0, x\eta + p > 0, p > 0 : u = [0, \underline{u_2}, \underline{u_3}]$$

$$\frac{x}{\eta} + p = 0, x\eta + p < 0, p < 0 : u = [undef, 0, 0]$$

$$\frac{x}{\eta} + p > 0, x\eta + p = 0, p < 0 : u = [0, undef, 0]$$

$$\frac{x}{\eta} + p > 0, x\eta + p > 0, p = 0 : u = [0, \underline{u_2}, undef]$$

Optimal control mode checking Kelley's condition to obtain first undefined operational mode $u = [undef, 0, 0]$.

$$\begin{aligned}\xi_1 &= \frac{\partial H}{\partial u_1} = \frac{x}{\eta} + p = 0 \\ \dot{\xi}_1 &= \frac{\dot{x}}{\eta} + \dot{p} \\ &= \frac{u_1 - (A + Bx^2)}{\eta} + \left(-\frac{u_1}{\eta} + 2Bxp\right) = -\frac{A + Bx(x - 2p\eta)}{\eta} = -\frac{A + 3Bx^2}{\eta} \\ \ddot{\xi}_1 &= \frac{\ddot{x}}{\eta} + \ddot{p} \\ &= \frac{A - 6B\dot{x}}{\eta} = -\frac{A + 6B(u_1 - f_{res}(x))}{\eta} \\ u_1 &= f_{res}(x) \\ (-1)^2 \frac{\partial}{\partial u_1} \frac{d^2}{dt^2} \xi_1 &= -\frac{A + 6Bu_1}{\eta} \leq 0\end{aligned}$$

Now the same strategy with the second case $u = [0, undef, 0]$

$$\begin{aligned}\xi_2 &= \frac{\partial H}{\partial u_2} = x\eta + p = 0 \\ \dot{\xi}_2 &= \dot{x}\eta + \dot{p} \\ &= u_2\eta - (A + Bx^2)\eta + (-u_2\eta + 2Bxp) = -A\eta - Bx(x - 2p\eta)\eta = -A\eta - 3Bx^2\eta \\ \ddot{\xi}_2 &= \ddot{x}\eta + \ddot{p} \\ &= -A\eta - 6B\dot{x}\eta = -\eta(A + 6B(u_2 - f_{res}(x))) \\ u_2 &= f_{res}(x) \\ (-1)^2 \frac{\partial}{\partial u_2} \frac{d^2}{dt^2} \xi_2 &= -\eta(A + 6B) \leq 0\end{aligned}$$

And finally for the last equation $u = [0, 0, \text{undef}]$

$$\xi_3 = \frac{\partial H}{\partial u_3} = p = 0$$

$$\dot{\xi}_3 = \dot{p}$$

$$= u_2 \eta + 2pBx = u_2 \eta \neq 0$$

As $u_2 \eta \neq 0$ this solution is infeasible, so this operational mode is removed from the final operational modes, which give us only 5 operational modes.